AN EXPERIMENTAL INVESTIGATION OF THE STABILITY OF POISEUILLE FLOW

by

Richard Evans Westbrook

United States
Naval Postgraduate School

THESIS

AN EXPERIMENTAL INVESTIGATION OF THE

STABILITY OF POISEUILLE FLOW

by

Richard Evans Westbrook

December 1969

An Experimental Investigation of the Stability of Poiseuille Flow

by

Richard Evans Westbrook
Lieutenant, United States Navy
B. S., United States Naval Academy, 1962

Submitted in partial fulfillment of the
requirements for the degrees of

MECHANICAL ENGINEER

and

MASTER OF SCIENCE IN MECHANICAL ENGINEERING

from the

NAVAL POSTGRADUATE SCHOOL
December 1969

ABSTRACT

A theoretical and experimental investigation of the stability of developing laminar flow in a circular pipe subjected to small, rotationally symmetric (torsional) disturbances is presented. Analytically, developing mean velocity profiles were represented in polynomial series form and subsequent formulations yielded determinations on stability which reduce to the classical conclusions for the case of fully developed flow.

Experimentally, torsional disturbances were imposed upon a developing laminar pipe flow by sinusoidally rotating a 1.5 inch (1 diameter) length of pipe in the entrance region of a carefully constructed wind tunnel facility. For flows with maximum Reynolds numbers of 8500, maximum amplitude and frequency of oscillation were ½ inch and 30 Hz., respectively. Hot wire anemometer measurements verified the stability of the developing flow field. Moreover, measured wave speeds and decay factors compare favorably to calculated values.

TABLE OF CONTENTS

I. INTRODUCTION - 11

II. THEORETICAL ANALYSIS - - - - - - - - - - - - - - - - - 13

A. CYLINDRICAL ORR-SOMMERFELD EQUATIONS - - - - - - - 13

B. DEVELOPING FLOW STABILITY DETERMINATIONS - - - - - - 16

III. EXPERIMENTAL ANALYSIS - - - - - - - - - - - - - - - - - 24

A. TUNNEL FACILITIES AND EXPERIMENTAL PROCEDURE - - - 24

B. TUNNEL PERFORMANCE AND EXPERIMENTAL RESULTS - - - 26

IV. CONCLUSIONS - 31

V. COMMENTS AND RECOMMENDATIONS - - - - - - - - - - - - - 33

BIBLIOGRAPHY - 35

INITIAL DISTRIBUTION LIST - - - - - - - - - - - - - - - - - - 36

FORM DD 1473 - 65

LIST OF TABLES

1 Coefficients of the Polynomial Approximations to the Velocity Profiles - - - - - - - - - - - - - - - - 37

LIST OF FIGURES

Figure

1 Drawing of Disturbance Generator - - - - - - - - - - - - 38

2 Developing Velocity Profile, z/d = 16, R = 5700 - - - - 39

3. Developing Velocity Profile, z/d = 56, R = 5700 - - - - 40

4. Developing Velocity Profile, z/d = 16, R = 8500 - - - - 41

5. Developing Velocity Profile, z/d = 56, R = 8500 - - - - 42

6. Radial Distribution of Disturbance Amplitude, z/d = 16, R = 5700 - - - - - - - - - - - - - - - - - - - 43

7. Radial Distribution of Disturbance Amplitude, z/d = 48, R = 5700 - - - - - - - - - - - - - - - - - - - 44

8. Radial Distribution of Disturbance Amplitude, z/d = 16, R = 8500 - - - - - - - - - - - - - - - - - - - 45

9. Radial Distribution of Disturbance Amplitude, z/d = 48, R = 8500 - - - - - - - - - - - - - - - - - - - 46

10. Radial Distribution of Disturbance Amplitude, z/d = 56, R = 5700 and R = 8500 - - - - - - - - - - - - 47

11. Radial Distribution of Disturbance Amplitude, z/d = 16, R = 5700 - - - - - - - - - - - - - - - - - - - 48

12. Radial Distribution of Disturbance Amplitude, z/d = 48, R = 5700 - - - - - - - - - - - - - - - - - - - 49

13. Radial Distribution of Disturbance Amplitude, z/d = 16, R = 8500 - - - - - - - - - - - - - - - - - - - 50

14. Radial Distribution of Disturbance Amplitude, z/d = 48, R = 8500 - - - - - - - - - - - - - - - - - - - 51

15. Radial Distribution of Distrubance Amplitude, z/d = 16, R = 5700 - - - - - - - - - - - - - - - - - - - 52

16. Radial Distribution of Disturbance Amplitude, z/d = 32, R = 5700 - - - - - - - - - - - - - - - - - - - 53

17. Radial Distribution of Disturbance Amplitude, z/d = 16, R = 5700 - - - - - - - - - - - - - - - - - - - 54

18. Radial Distribution of Disturbance Amplitude, z/d = 48, R = 5700 - 55

19. Radial Distribution of Disturbance Amplitude, z/d = 32, R = 8500 - 56

20. Radial Distribution of Disturbance Amplitude, z/d = 48, R = 8500 - 57

21. Radial Distribution of Disturbance Amplitude, z/d = 32, R = 8500 - 58

22. Polynomial Approximation to the Velocity Profile, z/d = 16, R = 5700 - - - - - - - - - - - - - - - - - - - 59

23. Polynomial Approximation to the Velocity Profile, z/d = 56, R = 5700 - - - - - - - - - - - - - - - - - - - 60

24. Polynomial Approximation to the Velocity Profile, z/d = 16, R = 8500 - - - - - - - - - - - - - - - - - - - 61

25. Polynomial Approximation to the Velocity Profile, z/d = 56, R = 8500 - - - - - - - - - - - - - - - - - - - 62

26. Decay of Disturbance Amplitude, R = 7600 - - - - - - - 63

27. Neutral Stability Curve - - - - - - - - - - - - - - - - 64

NOMENCLATURE

a_0, a_1, a_2, a_3, a_4	Constants, coefficients of the power series solution of the disturbance amplitude function
b_0, b_1, b_2, b_3	Constants, coefficients of the polynomial approximation of the velocity profile
C_r	Dimensionless wave speed
C_i	Amplification factor
d	Inside diameter of the pipe
P	Pressure
r	Radius of the pipe
R	Reynolds number ($R=\frac{Ud}{\nu}$)
$\overline{U}$	Mean velocity in the pipe
U_{max}	Maximum velocity in the pipe
U_o	Dimensionless velocity profile in the entry region, referred to U_{max}
u	Axial component of velocity
w	Tangential component of velocity
z	Axial coordinate
α	Disturbance wave number
ν	Kinematic viscosity
ψ	Stream function

ACKNOWLEDGEMENT

The author is deeply indebted to Professor T. Houlihan for his guidance and encouragement during the course of this investigation and to Professor T. Sarpkaya, without whom the work would not have been possible. A special note of appreciation is also given to Messrs. K. Mothersell, J. McKay, J. Beck, and G. Baxter of the Mechanical Engineering Machine Shop for their efforts and assistance in the construction of the apparatus.

I. INTRODUCTION

The purpose of the work reported here was the study of the evolution of small, rotationally symmetric disturbances introduced into the laminar transition region (the hydrodynamic entrance length) of Poiseuille pipe flow.

Since the pioneering work in the field of hydrodynamic stability conducted by O. Reynolds in the 1880's, the stability of fully developed pipe flow has been the subject of many theoretical and experimental studies. All of the analyses up to the present concerning the stability of fully developed pipe flow show that such a flow is stable to small disturbances.

A review of the theoretical and experimental determinations concerning the transition phenomenon leads one to the following considerations: (1) transition impends because the disturbances introduced contain some initially large disturbances so that small disturbances are not significant regardless of when or where they are introduced; or, (2) initially small disturbances, either axially-symmetric, rotationally symmetric or three-dimensional, grow in size along a favorable length of conduit, namely the entrance length, via convective interaction while the boundary layer is rapidly developing. Consequently, these small disturbances, which would not have grown in a fully developed region, now acquire a magnitude which eventually renders the fully developed flow unstable.

A theoretical analysis in support of the above considerations has been presented by Tatsumi [1]. His conclusions demonstrated that small disturbances magnified in the entrance region of a pipe flow field above

a minimum Reynolds number of 19,400, do cause transition after a passage of 17 tube radii. The significance of his study is not the determination of a value for the critical Reynolds number, but that there is a prediction of instability.

Presently, the case of developing axially-symmetric flow is treated. Results are shown to be reducible to the determinations of Pekeris [5] for fully developed pipe flow. Additionally, experimental verification of calculated wave speeds and amplification factors is presented.

II. THEORETICAL ANALYSIS

A. CYLINDRICAL ORR-SOMMERFELD EQUATIONS

To describe a general disturbance in mathematical form requires the formulation of a three-dimensional (r, $\emptyset$, z) vector function of time, t. The generally accepted treatment for small disturbances is to view them as a Fourier series of a large number of elementary disturbances, each of which can be represented in time and space by a finite number of parameters. Indeed, this is the foundation of the small disturbance theory - that the disturbance is a linear combination of spatially periodic components which grow or decay with time. Such a component is characterized by the stream function,

$$\Psi = F(r)\,\mathrm{Exp}\left[i n \emptyset + i \beta t - i \alpha z\right] \qquad (1)$$

By further contending that the imposed disturbance be rotationally symmetric, then the $\emptyset$ dependence is eliminated, and the representation reduces to,

$$\Psi = F(r)\,\mathrm{Exp}\left[i \alpha (Ct - z)\right] \qquad (2)$$

Therein α is a real number - the wave number of the disturbance in the fluid. C is a complex number, $C_r + iC_i$. The sign of the imaginary part of C, C_i, determines whether amplification ($C_i < 0$) or decay ($C_i > 0$) occurs, whereas C_r is the wave speed of the disturbance. Experimentally, such a disturbance is difficult to generate, since, as formulated, it should be imposed upon the entire length of the conduit over the entire cross-section of the conduit simultaneously, and very periodically in z as well.

Analytically, the disturbance described in (2) is thought of as being imposed upon a steady mean flow characterized by a stream function,

$$\psi_o = \psi(r,z) \tag{3}$$

The equations of motion for incompressible flow symmetric about the axis of a pipe are:

$$\frac{\partial v}{\partial t} + v\frac{\partial v}{\partial r} + u\frac{\partial v}{\partial z} = -\frac{1}{\rho}\frac{\partial p}{\partial r} + \nu\left[\nabla^2 v - \frac{v^2}{r}\right] \tag{4a}$$

$$\frac{\partial u}{\partial t} + v\frac{\partial u}{\partial r} + u\frac{\partial u}{\partial z} = -\frac{1}{\rho}\frac{\partial p}{\partial z} + \nu\nabla^2 u \tag{4b}$$

$$\frac{\partial v}{\partial r} \quad \frac{v}{r} \quad \frac{\partial u}{\partial z} = 0 \tag{4c}$$

$$\nabla^2 = \frac{\partial^2}{\partial r^2} + \frac{1}{r}\frac{\partial}{\partial r} + \frac{\partial^2}{\partial z^2} \tag{4d}$$

It is convenient to introduce the non-dimensional coordinates,

$$r' = \frac{r}{d}\ ,\ z' = \frac{z}{d}\ ,\ t' = \frac{t\bar{U}}{d}\ ,\ p' = \frac{p}{\rho\bar{U}^2}\ ,$$

and define R, the Reynolds number as $R = \frac{Ud}{\nu}$. With these substituted, the system of equations (4) becomes:

$$\frac{\partial v'}{\partial t'} + v'\frac{\partial v'}{\partial r'} + u'\frac{\partial v'}{\partial z'} = -\frac{\partial p'}{\partial r'} + \frac{1}{R}\left[\nabla^2 v' - \frac{v'^2}{r'}\right] \tag{5a}$$

$$\frac{\partial u'}{\partial t'} + v'\frac{\partial u'}{\partial r'} + u'\frac{\partial u'}{\partial z'} = -\frac{\partial p'}{\partial z'} + \frac{1}{R}\nabla^2 u' \tag{5b}$$

$$\frac{\partial v'}{\partial r'} + \frac{v'}{r'} + \frac{\partial v'}{\partial z'} = 0 \qquad (5c)$$

Defining $U = \frac{1}{r}\frac{\partial \psi}{\partial r}$ and $V = -\frac{1}{r}\frac{\partial \psi}{\partial z}$, it is noted that with the dependence on $\emptyset$ dropped, that there are two possible types of symmetrical disturbances which may be generated and which are not mathematically coupled. First, there exist the torsional disturbances, which are concentric with respect to the pipe axis; secondly, there exist the meridional disturbances, which occur in planes passing through, and parallel to, the axis of the pipe. Treatment of each case is necessary due to the aforementioned difficulty in experimentally imposing the mathematically exact disturbance upon a flow regime. It is assumed that,

$$\psi'(r,z,t) = f(r)\,\mathrm{Exp}\left[i\alpha(Ct - z)\right] \qquad (6a)$$

$$\Omega(r,z,t) = G(r)\,\mathrm{Exp}\left[i\alpha(Ct - z)\right] \qquad (6b)$$

These relations, together with the definitions of velocity components in terms of the stream functions, lead to the following uncoupled system of <u>exact</u> equations of motion:

$$\frac{\partial}{\partial t}D^2\psi + 2\frac{\Omega}{r^2}\frac{\partial \Omega}{\partial z} + \frac{1}{r}\left[\frac{\partial \psi}{\partial z}\frac{\partial}{\partial z}D^2\psi - \frac{\partial \psi}{\partial z}\frac{\partial}{\partial r}D^2\psi\right] + \frac{2}{r^2}\frac{\partial \psi}{\partial z}D^2\psi = \frac{1}{R}D^4\psi \qquad (7a)$$

$$\frac{\partial \Omega}{\partial t} + \frac{1}{r}\left[\frac{\partial \psi}{\partial r}\frac{\partial \Omega}{\partial z} - \frac{\partial \psi}{\partial z}\frac{\partial \Omega}{\partial r}\right] = \frac{1}{R}D^2\Omega \qquad (7b)$$

where $D^2 = \frac{\partial^2}{\partial r^2} - \frac{1}{r}\frac{\partial}{\partial r} + \frac{\partial^2}{\partial z^2}$

As ψ is composed of the main flow with the disturbance superimposed upon it, it can be described as,

$$\Psi = \Psi_0 + \Psi' \tag{8}$$

where Ψ_0 refers to the main flow and Ψ' is as defined in (6a). Substituting (8) into the system (7), dropping squares and products of Ψ' and Ω, as each is assumed small, leads to the following uncoupled system of linearized equations:

$$\frac{\partial}{\partial t} D^2\Psi' + \frac{1}{r}\left[\frac{\partial \Psi_0}{\partial r}\frac{\partial}{\partial z} D^2\Psi' + \frac{\partial \Psi'}{\partial r}\frac{\partial}{\partial z} D^2\Psi_0 - \frac{\partial \Psi_0}{\partial z}\frac{\partial}{\partial r} D^2\Psi' - \frac{\partial \Psi'}{\partial z}\frac{\partial}{\partial r} D^2\Psi_0\right] \tag{9a}$$

$$+ \frac{2}{r^2}\left[\frac{\partial \Psi_0}{\partial z} D^2\Psi + \frac{\partial \Psi'}{\partial z} D^2\Psi_0\right] = \frac{1}{R} D^4\Psi'$$

$$\frac{\partial \Omega}{\partial t} + \frac{1}{r}\left[\frac{\partial \Psi_0}{\partial r}\frac{\partial \Omega}{\partial z} - \frac{\partial \Psi_0}{\partial z}\frac{\partial \Omega}{\partial r}\right] = \frac{1}{R} D^2\Omega. \tag{9b}$$

To proceed further requires that the exact nature of Ψ_0 be known. In the fully developed case, Ψ_0 is a simple function of r alone, and is easily treated. In the case of developing flows, such as the one under investigation, there is no precise, known functional description of,

$$\Psi_0 = \Psi_0(r, z, t).$$

B. DEVELOPING FLOW STABILITY DETERMINATIONS

Schiller [2], and Langhaar [3] present workable models of developing velocity profiles in parametric form. However, after long and fruitless attempts, the author has concluded that there is no simplified mathematical solution suitable for representation of the developing mean flow at present. Accordingly, following Tatsumi [1], purely parallel flows which have the same velocity profile at a given axial distance as the developing flow shall be treated. For such velocity profiles, it was found that experimental data could be approximated to an excellent degree of

accuracy by a third degree polynomial obtained from a least-squares curve fitting procedure. To make the solution more general, it is assumed that

$$U_0(r) = b_0 + b_1 r + b_2 r^2 + b_3 r^3 \quad (10)$$

from which

$$\psi_0(r) = \frac{b_0 r^2}{2} + \frac{b_1}{3} r^3 + \frac{b_2}{4} r^4 + \frac{b_3}{5} r^5 \quad (11)$$

is obtained. By obtaining the necessary terms from (11) and (6) and substituting them into (9), the following equations are obtained:

$$D^2 g = i\alpha R\left[\left(C - b_0 - b_1 r - b_2 r^2 - b_3 r^3\right) g + \left(3b_3 - \frac{b_1}{r}\right) f\right] \quad (12a)$$

where

$$g \equiv f'' - \frac{f'}{r} - \alpha^2 f \quad (12b)$$

and primes denote differentiation with respect to r. Treating (12a) first, it is clear that for large R, the terms on the right side of the equation will predominate, since even when α is assumed small, αR is still large. Yet, if the entire $D^2 g$ term is ignored, it is impossible to satisfy all of the boundary conditions of the problem. Order of magnitude considerations allow for the retention of the g'' term, and thus satisfaction of all boundary conditions. Returning to the definition of g,

$$g'' = f^{IV} - \frac{1}{r} f''' + \left(\frac{2}{r^2} - \alpha^2\right) f'' - \frac{2}{r^3} f' \quad (13)$$

Inserting (13) into (12b) then yields,

$$f^{IV} - \frac{1}{r} f''' + \left(\frac{2}{r^2} - \alpha^2 - R\sigma_g\right) f'' + \left(-\frac{2}{r^3} + \frac{R}{r}\sigma_g\right) f' + \left[\alpha^2 R\sigma_g - i\alpha R\sigma_f\right] f = 0 \quad (14)$$

where

$$\sigma_g = i\alpha\left(C - b_0 - b_1 r - b_2 r^2 - b_3 r^3\right)$$

and

$$\sigma_f = i\alpha\left(3b_3 r - \frac{b_1}{r}\right)$$

Before simplification, equation (14) is of the general form,

$$y^{IV} + P(r)\,y''' + Q(r)\,y'' + R(r)\,y' + T(r)\,y = 0$$

a form which possesses a regular singular at the origin, r = 0. This fact guarantees the existence of at least one series solution of the form

$$f(r) = r^m \sum_{k=0}^{\infty} a_k r^k \tag{15}$$

which will converge for $0 < r < r_o$, where r_o is the distance from the origin to the next nearest singular point. As the disturbances introduced are confined to the vicinity of the pipe wall, $r \sim 1$, and again following Schlichting [6], the terms

$$\frac{1}{r} f''' \;,\; \frac{2}{r^2} f'' \;,\; -\alpha^2 f'' \quad \text{and} \quad \frac{2}{r^3} f'$$

are neglected as they are all of the order 1, whereas the αR term is assumed quite large. The resultant equation is

$$f^{IV} - R\sigma_g f'' + R\sigma_g \frac{f'}{r} + (\alpha^2 R\sigma_g - R\sigma_f) f = 0 \tag{16}$$

Assuming a solution of the form (15), differentiating and inserting terms,

$$\sum_{k=0}^{\infty} (m+k)(m+k-1)(m+k-2)(m+k-3)\, a_k\, r^{m+k-4}$$

$$- i\alpha R \left[\sum_{k=0}^{\infty} (m+k)(m+k-1) a_k r^{m+k-2} \right] (C - b_0 - b_1 r - b_2 r^2 - b_3 r^3) \tag{17}$$

$$+ i\alpha R \left[\sum_{k=0}^{\infty} (m+k) a_k r^{m+k-2} \right] (C - b_0 - b_1 r - b_2 r^2 - b_3 r^3)$$

$$+ i\alpha R \left[\sum_{k=0}^{\infty} a_k r^{m+k} \right] \left(\alpha^2 (C - b_0 - b_1 r - b_2 r^2 - b_3 r^3) - \left(3b_3 r - \frac{b_1}{r} \right) \right) = 0$$

Setting the coefficient of the highest power of r equal to zero results in the indicial equation,

$$n(n-1)(n-2)(n-3)a_0 = 0$$

with indicies n = 0,1,2,3 to guarantee that $a_0 \neq 0$.

Before proceeding further, specific attention is due to the boundary conditions of the problem. The no slip condition at the wall guarantees that f'(1) = 0, i.e., $\frac{1}{r}\frac{\partial \psi}{\partial r} = 0$. Since the flow is axially symmetric, v' must be symmetric, hence zero on the axis, or f(0) = 0. Finally, there can be no sources at the wall, and therefore $\psi'(1) = 0$, or f(1) = 0. Here, it should be noted that most previous works also include a condition that u'(0) = 0, or that f'(0) = 0. However, as noted by Leite [4], there is no guarantee that only those disturbances generated by the experimenter are being accepted by the flow, i.e., there is no a priori reason to expect u'(0) = 0. It is noteworthy that it is not necessary to impose this artificial condition in this analysis.

Taking the largest exponent of r first, it is found that the second highest ordered coefficient,

$$(n-1)(n)(n+1)(n+2)a_1 = 0 \tag{18}$$

can only be identically satisfied of $a_1 = 0$. Continuing, for each coefficient in turn, it is found that the recurrance relation yields:

$$a_2 = \frac{i\alpha R(c-b_0)(n-2)}{(n+2)(n+1)(n-1)} \tag{19}$$

$$a_3 = -\frac{i\alpha R b_1 (n-1)^2}{(n+3)(n+2)(n+1)n} a_0 \tag{20}$$

$$a_4 = \frac{i\alpha R\, a_0}{(n+4)(n+3)(n+2)(n+1)}\left[\frac{i\alpha R(C-b_0)^2 n(n-2)}{(n+1)(n-1)} - n(n-1)b_2 + \alpha^2(C-b_0)\right] \quad (21)$$

After substituting n = 3, then;

$$a_2 = \frac{a_0}{40}\, i\alpha R(C-b_0) \qquad \text{and} \qquad a_3 = -\frac{a_0}{90}\, i\alpha R\, b_1$$

$$a_4 = \frac{a_0}{840}\left[\frac{3}{8}\left(i\alpha R(C-b_0)\right)^2 - i\alpha R\left(3b_2 + \alpha^2(C-b_0)\right)\right]$$

With these coefficients, the final form of the solution becomes,

$$f(r) = a_0 r^3\left[1 + \frac{r^2}{40} i\alpha R(C-b_0) - \frac{r^3}{90} i\alpha R\, b_1 - \frac{r^4}{840}\left(\frac{3}{8}\alpha^2 R^2 (C-b_0)^2 - i\alpha R\left(3b_2 + \alpha^2(C-b_0)\right)\right)\right] \quad (22)$$

The existence of additional linearly independent solutions is determined by returning to the indicial equation. The value n = 0 will yield such a solution, but as the boundary condition f(0) = 0 would not be satisfied without $a_o = 0$, then this solution may be discarded. The same consideration applies for the value n = 1, i.e., the f'(1) = 0 boundary condition would not be satisfied without $a_o = 0$. In each of these cases, if a_o were to be equal to zero, then it is evident that the series could be represented as

$$\sum_{k=0}^{\infty} a_{k+1}\, r^{m+k+1}$$

Therein, the values n = 0 and n = 1 would not then satisfy the resultant indicial equation.

Finally, the case of n = 2, the last of the four index values is considered. Now, n = 2 identically satisfies the recurrance relation involving a_1, i.e., the second highest ordered term. Thus, it is possible that this value would yield a linearly independent solution.

However, as this exponent differs from the highest by a positive integer (vis. 1), it is always possible to generate another linearly independent solution of the form[1],

$$\sum_{k=0}^{\infty} c_k r^{m+k} + \ln(r) \sum_{k=0}^{\infty} d_k r^{m+k}$$

This solution clearly fails the f(0) = 0 boundary condition, hence it is also discarded. Therefore, of the four linearly independent solutions possibly generated by the exponents from (18), only one remains that satisfies all the conditions of the problem, viz., the solution represented in relation (22).

Applying first the wall boundary condition to this solution yields,

$$f(r) = 1 - \frac{\alpha R}{40} C_i + \frac{\alpha^3 R}{840} C_i - \frac{3\alpha^2 R^2}{8.840}\left[(C_R - b_0)^2 - C_i^2\right] + \frac{i\alpha R}{40} C_R - b_0 - \frac{i\alpha R b_1}{90} - \frac{i\alpha R b_2}{840} - \frac{i\alpha R (C_R - b_0)}{840} - \frac{3}{4.840} i\alpha^3 R^2 C_i (C_R - b_0) = 0 \quad (23)$$

Separating this equation into real and imaginary parts gives

$$C_R - b_0 - \frac{b_1}{90} - \frac{3b_2}{840} - \frac{\alpha^2 (C_R - b_0)}{840} - \frac{3\alpha R C_i (C_R - b_0)}{4.840} = 0 \quad (24a)$$

$$1 - \frac{\alpha R C_i}{40} + \frac{\alpha^3 R C_i}{840} - \frac{3\alpha^2 R^2}{8.840}\left[(C_R - b_0)^2 - C_i^2\right] = 0 \quad (24b)$$

Solving (24a) for C_i results in

$$C_i = \frac{28}{\alpha R} - \frac{12.45\, b_1}{\alpha R (C_R - b_0)} - \frac{4 b_2}{\alpha R (C_R - b_0)} - \frac{4\alpha^2}{3\alpha R} \quad (25)$$

---

[1] Hildebrand, F. B., Operational Calculus for Applications, p. 137, Prentice-Hall, 1962.

Following the same procedure as above in applying the boundary condition $f'(1) = 0$ to the solution in relation (22) yields two additional equations

$$\frac{C_R - b_0}{8} - \frac{b_1}{5} - \frac{b_2}{40} - \frac{\alpha^2 (C_R - b_0)}{120} - \frac{\alpha R C_i (C_R - b_0)}{160} = 0 \quad (26a)$$

$$3 - \frac{\alpha R C_i}{8} + \frac{\alpha^3 R C_i}{120} - \frac{\alpha^2 R^2}{320}\left[(C_R - b_0)^2 - C_i^2\right] = 0 \quad (26b)$$

Solving (26a) for C_i gives

$$C_i = \frac{20}{\alpha R} - \frac{32 b_1}{\alpha R C_R - b_0} - \frac{4 b_2}{\alpha R C_R - b_0} - \frac{4\alpha^2}{3\alpha R} \quad (27)$$

It should be noted that C_i and C_r have each been normalized with respect to U_{max} and that α has been normalized with respect to d. It is clear that the normalized C_r value, the wave speed, takes on values $0 \leq C_r \leq 1$ with the maximum value occurring in the region of maximum flow velocity. Inspection of (25) and (27) reveals that, within the developing region, C_i must always be positive. Hence the developing region is stable. Further, in the limiting case, viz., in the fully developed flow regime, the coefficients of the polynomial representation of the velocity profile become;

$$b_o = 1,\ b_3 = -1,\ b_2 = b_4 = 0$$

Analagous considerations demonstrate then that in the limiting case of fully developed flow, the solution represented by (22) also holds.[1]

---

[1] See Also reference [5].

Data obtained from the curve fitting procedure is presented later to verify the applicability of this solution to the developing flow regime. The solution of (24b) would follow from Pekeris [5] under the assumption of purely parallel flows. Further pursuit of the exact solution of (24b) however, depends on the exact determination of v as a function of r and z.

III. EXPERIMENTAL ANALYSIS

A. TUNNEL FACILITIES AND EXPERIMENTAL PROCEDURE

The experiments were conducted in a horizontal Lucite pipe 1.5 inches I.D. and 45 feet (300 diameters) long. A centrigugal fan was used to pull air from the stagnation conditions in the plenum chamber through the system. The inlet chamber consisted of a rectangular box 3 feet square in cross-section and 4 feet long which was fitted internally with 6-24 mesh wire screens, followed by a 2 foot long settling chamber. Sizing of the chamber was fixed to limit the maximum interior velocity to 1.5 fps. The well rounded inlet horn was a quarter-section of a 9 inch by 18 inch ellipse molded of fiber glass and polished smooth. All joints were hand fitted to insure smoothness and uniformity of mating interior surfaces.

The disturbance generator, Figure 1, was located 12 inches (8 diameters) from the pipe entrance, and was followed by measuring ports at 16, 20, 32, 40, 48, 56, and 272 diameters downstream of the entrance. Uniformity of the internal diameter and concentricity of the pipe were found to be within .005 inch for all sections of the pipe. The individual pipe sections were joined by flanges, each pair hand fitted and joined to insure uniformity. The pipe sections joined to the disturbance generator were fitted with rubber O-rings to assist in damping any vibrations which might carry over from the driver to the pipe. The pipe was fastened to a horizontal metal track which was bolted to the concrete deck. The vibrator was securely fastened to the deck after being isolated with one inch of corrugated rubber vibration mounting. The entire apparatus was longitudinally aligned with a high power transit

and leveled. Maximum deviation from true horizontal and longitudinal alignment is felt to be no more than .25 inch over the entire length.

Measurements were taken with a Thermo-Systems constant temperature hot wire anemometer utilizing a boundary-layer type probe with a .095 inch long, .00015 inch diameter tungsten element. The probe could be located at any of the above mentioned stations, and accurately positioned to within .050 inch of the pipe wall.

Prior to the commencement of data-taking, a careful survey was taken to determine the physical limitations of the apparatus. It was found that the maximum attainable Reynolds number was 9650; however, at this setting, the sensitivity of the flow regime was such that any disturbance within the laboratory was sufficient to cause transition of the flow. The maximum usable Reynolds number was found to be 8500. The survey further revealed that above a frequency of oscillation of 30 Hz., too much vibration was being carried over to the conduit. Hence data runs were limited to oscillations at 30 Hz. and less.

The following procedure was used in taking data during the experimental phase:

1. The mean velocity corresponding to the desired Reynolds number was measured and monitored at the station located in the fully developed flow region (272 diameters from the entrance) by regulating the amount of air pulled by the fan.

2. The probe was positioned at the station nearest the generator, and rotated until the position fixing the maximum reading was found.

3. A velocity profile was first obtained; data taking runs then commenced with oscillation frequencies of 30 Hz., with ½ and ¼ inch amplitudes, oscillations then at 20 Hz., with ½ and ¼ inch amplitudes, and finally at 10 Hz at ½ inch amplitude.

4. The probe was then moved to the next location down stream, and steps 2 and 3 repeated.

5. Upon completion of recordings at all stations in the entry length region at the desired Reynolds number, step 1 followed by 2, 3 and 4 were again repeated for another Reynolds number.

The following procedures were used in recording data:

1. The output of the hot wire was displayed on an RMS meter and on a dual beam oscilloscope, as was the signal input to the vibrator.

2. As the probe was moved from its closest proximity to the wall towards the center of the tube in .025 inch increments, the hot wire bridge voltage and RMS voltage were recorded and the oscillogram either described or photographed. This step was repeated at each location for each data run conducted in (3) above.

The data obtained in the manner just described was normalized through the use of appropriate values. Graphical presentations of this data are discussed in the following sections of this report.

B. TUNNEL PERFORMANCE AND EXPERIMENTAL RESULTS

1. Developing Velocity Profiles

Figures 2 - 5 show the velocity profiles obtained both at high and low Reynolds numbers at two points in the developing flow. They are compared with the analytical approximations of Langhaar [2], with a correction factor of .8 applied to the development length. The correction factor was introduced because, similarly to Leite [3], it was found that the peak velocity obtained at a given axial location was always higher than that predicted by theory. It is additionally noted that the boundary layer itself does not develop as rapidly as predicted, although this factor is strongly dependent upon Reynolds number and thus may be a

characteristic of the apparatus. Figures 22 - 25 show the polynomial fitted by a least-squares technique, the results of which were used in the determination of the damping factor. The second curve in each of these figures is that of a fully developed profile offered for comparison. Table 1 contains a listing of the coefficients of the polynomials used.

The noise level in the developing flow is very much greater, by approximately an order of magnitude, than that previously reported in fully developed flow experiments. It is felt that due to the type of probe utilized and because of it's orientation, some of the noise signal is indeed a measure of the radial component of velocity, v. In any case, the average turbulence level for all stations was .8 - 1.0%. As might be expected, the higher values occurred at close proximity to the wall, and the minimum value was found in the core region of the profile. The very nature of the hydrodynamic entry region, where most of the frictional losses are known to occur in pipe flow, suggest that one should expect a rather noisy signal.

2. The Disturbance

At the highest frequency and highest amplitude, the turbulence level jumped to a peak of 12% near the wall, with the peak at the center line of 8% at the farthest station located in the entry length. At the highest Reynolds number tested, the level at the station in the fully developed region reached a peak value of 1.0% compared with .8% without any disturbance. It was noted that at all Reynolds numbers and at frequencies and amplitudes accepted by the flow, that the radial propagation of the disturbance was strongly dependent upon the velocity profile, i.e., upon the boundary layer thickness. Penetration into the core region was strongly amplitude dependent.

a. Reynolds Number Dependence

One would expect that, for a fixed frequency and amplitude, the level of turbulence at any downstream position along the pipe would increase with increasing Reynolds number. Figures 6 - 9 show plots of Turbulence Level vs. r/a at near and far stations at high and low Reynolds numbers and demonstrate this relation quite well. Figure 10 shows the confining effect of the thinner boundary layer found at higher Reynolds numbers, i.e., the higher level disturbances are not allowed to diffuse towards the center into the core region. This effect decreases dramatically with decreasing Reynolds number. Not only is diffusion allowed, but it occurs sooner, as the lower mean velocity would indicate. Lastly it is noted that there were combinations of frequencies and amplitudes which produced extremely small fluctuations in the mean flow, just above the background noise level. Such phenomenon were observed at 10 Hz. at an amplitude of ½ inch and at 20 Hz. at ¼ inch at all Reynolds numbers. It appears that these disturbances were simply damped within the boundary layer without producing the characteristic turbulent spike near the wall.

b. Frequency Dependence

Figures 11 - 14 show the very pronounced dependence of turbulence level upon the frequency of the disturbance generator. It is noted that as frequency is lowered, the speed at which the wave travels down the pipe should decrease. Hence the station at which a particular level of turbulence occurs for a given amplitude of disturbance at a given Reynolds number should be located further up stream as disturbance frequency is lowered. This is clearly shown in Figure 15. The idea of wave speed varying directly with the excitation frequency would seem to

suggest that, since the low frequency disturbance spends more time within the boundary layer, it interacts for a longer period with the strong viscous forces acting there. Hence it is damped more quickly and completely. Again the observation that the velocity profile itself strongly effects the characteristics of the disturbance in the fluid is apparent.

c. Amplitude Dependence

Figures 16 - 19 show the increase in turbulence with amplitude at low and high Reynolds numbers. Figure 20 shows the strong dependence of diffusion upon amplitude, i.e., at higher amplitudes, for a given Reynolds number and frequency of disturbance, the higher the amplitude of disturbance, the greater the penetration of the disturbance into the core. Lastly, the fact that damping occurs at the frequencies and amplitudes tested suggests that there is an amplitude below which all traces of the disturbance would damp over a distance of a few diameters. Such a determination was not made here, but its existance is foreshadowed.

3. The Damping Factor

Following Leite [4], it is seen that from the definition of the u component of velocity and from (6a),

$$\frac{U_1'}{U_2'} = EXP\left[-\int_{t_1}^{t_2} \alpha C_i \, dt\right] \tag{28}$$

If a suitable starting point, z_o, is chosen, this relation becomes,

$$\frac{U'}{U_o'} \quad EXP\left[-\int_{t(z_o)}^{t(z)} \alpha C_i \, dt\right] \tag{29}$$

or,

$$2.3 \, LOG_{10} \frac{U'}{U_o'} = -\int_{t(z_o)}^{t(z)} \alpha C_i \, dt \tag{30}$$

Thus,

$$C_i = \frac{2.3\, C_R}{\alpha} \frac{d}{dz}\left[LOG_{10} \frac{U'}{U_o'} \right]. \qquad (31)$$

If values of $LOG_{10} \frac{u'}{u'_o}$ are plotted vs. the downstream displacement $(z - z_o)/d$, the slopes of these curves will be,

$$\frac{d}{dz}\left[LOG_{10} \frac{U'}{U_o'} \right].$$

Then, if either a value of wave speed, C_r, or a value of wave number, α, can be determined, then C_i can easily be computed. As a check, equations 25 and 26 can then be solved to yield comparative values. Figure 26 shows a plot of $LOG_{10} \frac{u'}{u_o}$ vs. $(z - z_o)/d$ for data taken at Reynolds number of 7600 at the maximum frequency and two amplitudes. As one would expect, the slopes increase as the center of the pipe is approached. Further, at an r/a of .9, the larger disturbance is damped at a faster rate.

Equations 24 were solved utilizing several experimentally obtained velocity profiles. Results are presented in Figure 27, which portrays the characteristic "hairpin" neutral stability curve. Plots are also presented for C_i values of .05 and .1 which verify the stability of the flows tested.

IV. CONCLUSIONS

(1) Flow in the laminar transition region of a pipe of circular cross-section is stable to small, rotationally symmetric (torsional) disturbances.

(2) There exists a strong dependence of amplification factor and wave propagation speed upon the shape of the developing velocity profile.

(3) There is a dependence of both wave speed, C_r, and wave number, α_j upon radial position, though evaluation of this relationship will require an accurate description of v(r).

(4) Within the range of frequencies and amplitudes tested, there existed a peak turbulence level in excess of 10% very close to the wall of the pipe. However, disturbances of this magnitude never reached the core of the flow and transition of complete turbulence never occurred.

(5) Low frequency disturbances are completely damped within the developing boundary layer.

(6) The experimental results suggest the existence of a "critical layer" wherein the disturbance is sufficiently strengthened to cause transition to impend. Without this sufficient amplification, the disturbance diffuses into the central flow region, while continually being damped.

(7) Small disturbance theory per se plays only a small role in the overall description of the transition of pipe flows from the laminar to the turbulent state. Better understanding of this transition phenomenon can only be achieved through an analysis which would describe the spatial growth of a finite disturbance rather than the temporal growth or decay of an infinitesimal disturbance. However, even the latter, if amplified

by the flow regime, quickly reaches an amplitude beyond which linearization of the equations of motion is no longer possible. Hence, there is at present no mathematical method suitable for a truely comprehensive study of transition. It appears then that further experimental studies are the methods whereby more information can be gathered on this subject.

V. COMMENTS AND RECOMMENDATIONS

The experimental apparatus proved functional, easily maintained and operated, and very reliable. It is recommended that further pursuit of this experiment be preceeded by the following alterations:

(1) Construction of a new entrance section in accordance with the design of Cohen and Ritchie [8] to facilitate flow developing at very high Reynolds numbers.

(2) Extension of the pipe to allow fully developed flow to be achieved at Reynolds number of order 15,000.

(3) Integration of the air supply into a totally closed system to remove the possibility of interference from air currents and temperature variations within the laboratory.

(4) Modification of the disturbance generator itself for use of frequencies above 30 Hz. and amplitudes of $\frac{1}{2}$" from the present mechanical design to an electromagnetic design to eliminate vibration problems.

After improvements are made to the apparatus, prior to the resumption of experiments in stability, it is strongly recommended that an experimental study of developing pipe flow itself be undertaken to determine:

(1) The developing velocity components u and v as functions of the pertinent geometric parameters r and z.

(2) An analytical or numerical solution of the pertinent Orr-Sommerfeld equation.

It is the author's belief that the study of the stability problem itself utilizing the small disturbance theory will ultimately lead to a better understanding of the problem of beginning of transition from

laminar to turbulent flow. Such a study, however, must utilize analytical approaches more compatible with experimental procedure than those presented in the past.

BIBLIOGRAPHY

1. Tatsumi, T. J., Phy. Soc. of Japan, 7, p. 489, 1952.

2. Goldstein, S., Modern Developments in Fluid Dynamics, 1965.

3. Langhaar, H. L., J. Appl. Mech., 9, p. 55, 1942.

4. Leite, R. J., J. Fluid Mech., 5, p. 81, 1959.

5. Pekeris, C. L., Proc. Nat. Acad. Sci., Wash., 34., p. 285, 1948.

6. Schlichting, H., Boundary Layer Theory, McGraw-Hill, 1960.

7. Hildebrand, F. B., Advanced Calculus for Applications, Prentice-Hall, 1962.

8. Cohen, M. J. and N. J. B. Ritchie, J. Royal Aero. Soc., 66, p. 231, 1962.

INITIAL DISTRIBUTION LIST

		No. Copies
1.	Defense Documentation Center Cameron Station Alexandria, Virginia 22314	20
2.	Library, Code 0212 Naval Postgraduate School Monterey, California 93940	2
3.	Naval Ship Systems Command, Code 2052 Via Code 31 Department of the Navy Washington, D. C. 20360	1
4.	Mechanical Engineering Department Naval Postgraduate School Monterey, California 93940	2
5.	Professor T. M. Houlihan Mechanical Engineering Department Naval Postgraduate School Monterey, California 93940	3
6.	LT R. E. Westbrook, USN 16 Kingston Avenue Poughkeepsie, New York 12603	2

TABLE 1

Coefficients of the polynomial approximations to the velocity profiles at $z/d = 16$ and $z/d = 56$

z/d	Reynolds number	b_o	b_1	b_2	b_3
16	8500	.702197	-.752768	2.75123	-2.63370
16	5700	.733547	-.657861	2.64586	-2.7294
56	8500	.823472	-.378369	1.89644	-2.34190
56	5700	.87101	-.601644	2.70048	-3.02695

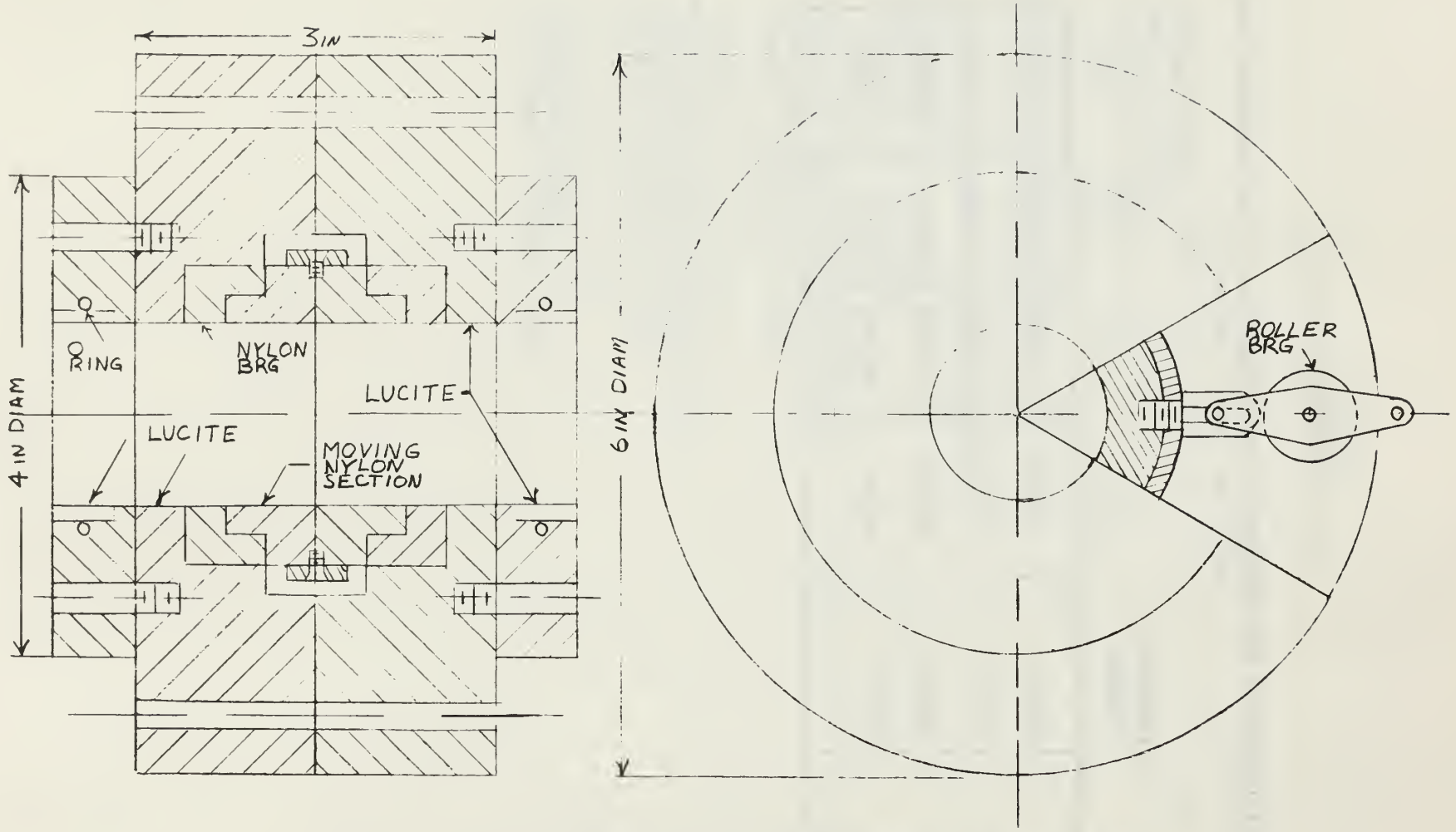

FIG 1 DISTURBANCE GENERATOR

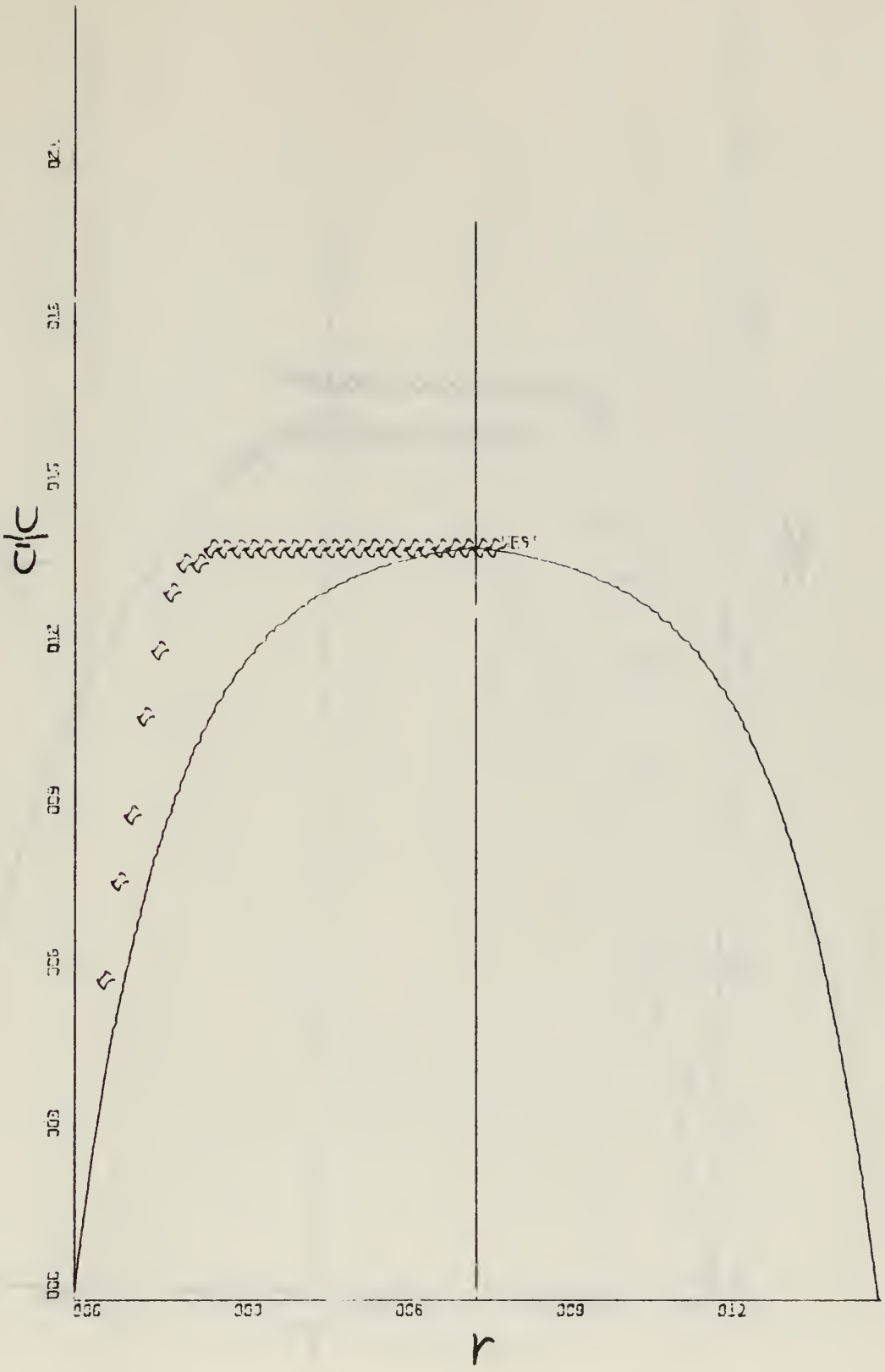

Figure 2: Developing Velocity Profile; z/d 16, R 5700

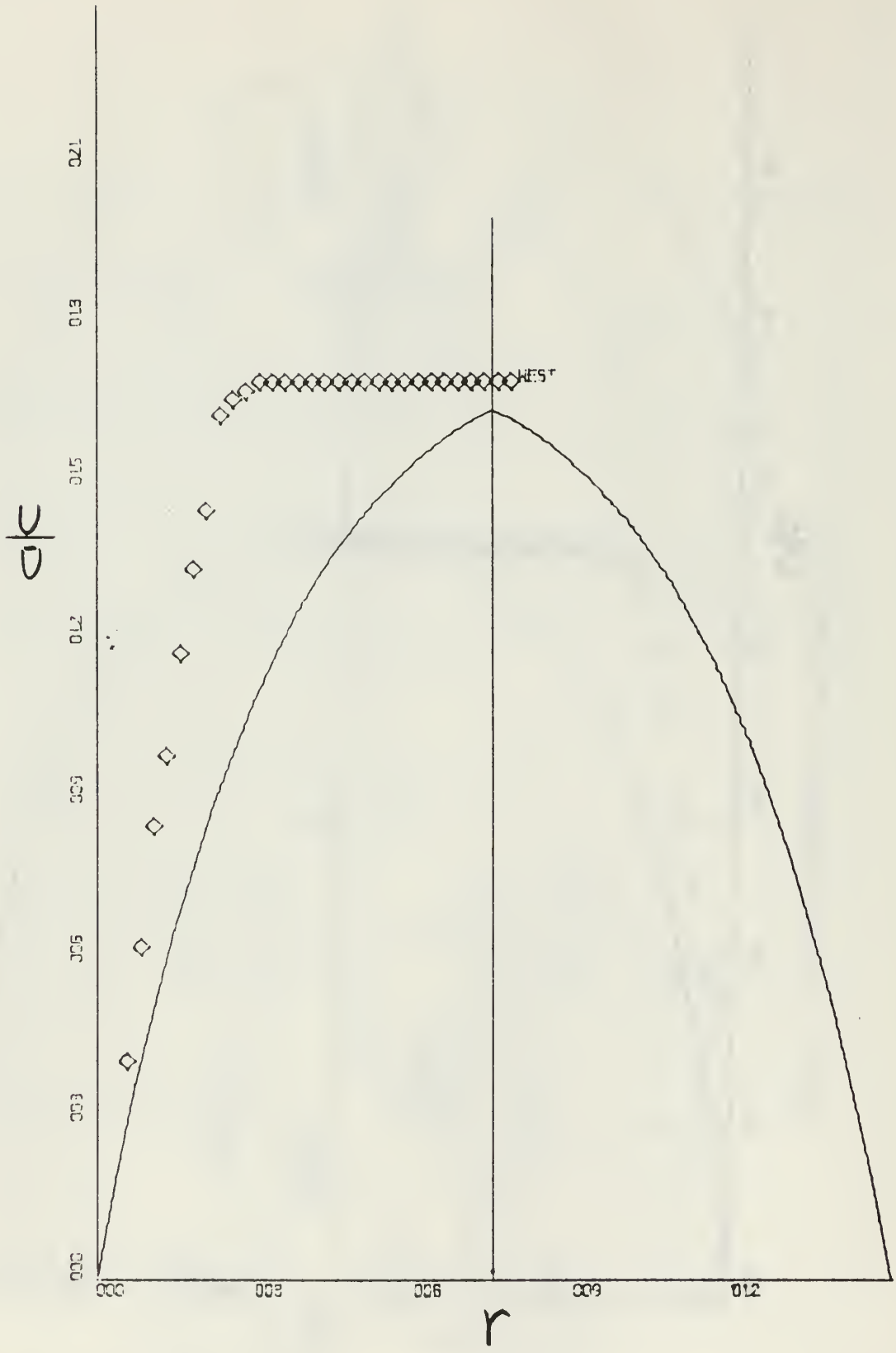

Figure 3: Developing Velocity Profile; z/d 56, R 5700

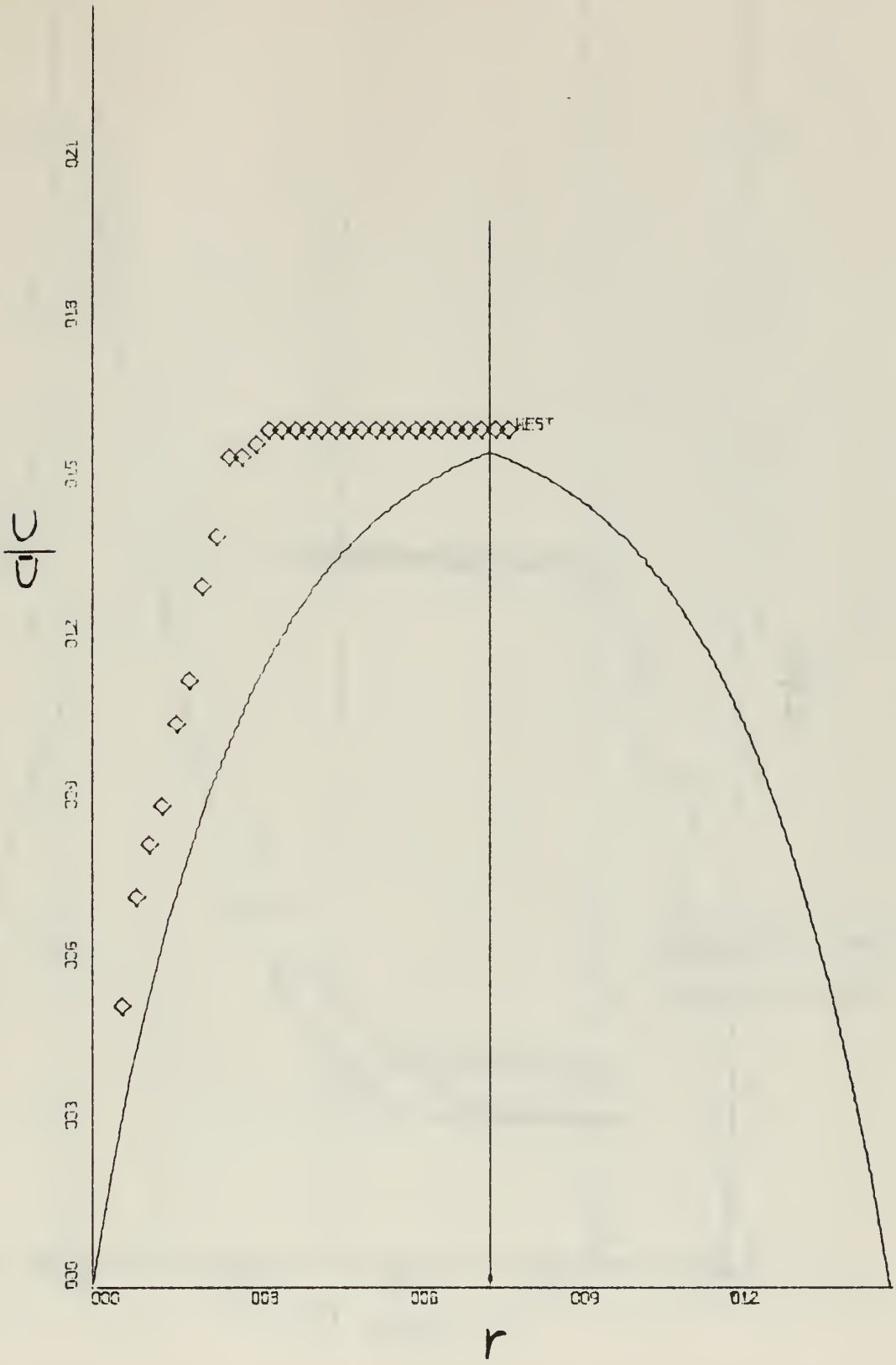

Figure 4: Developing Velocity Profile; z/d 16, R 8500

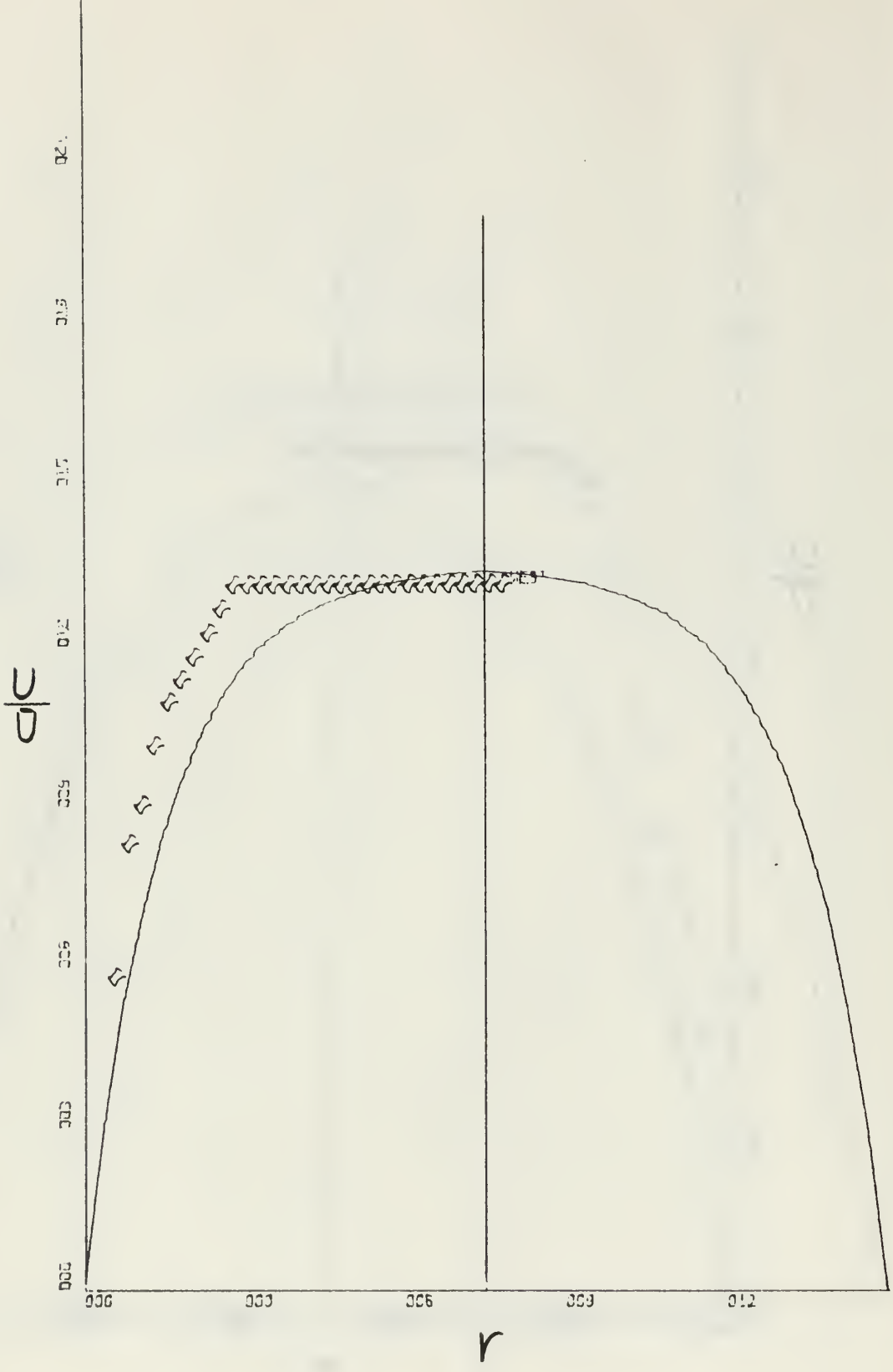

Figure 5: Developing Velocity Profile; z/d 56, R 8500

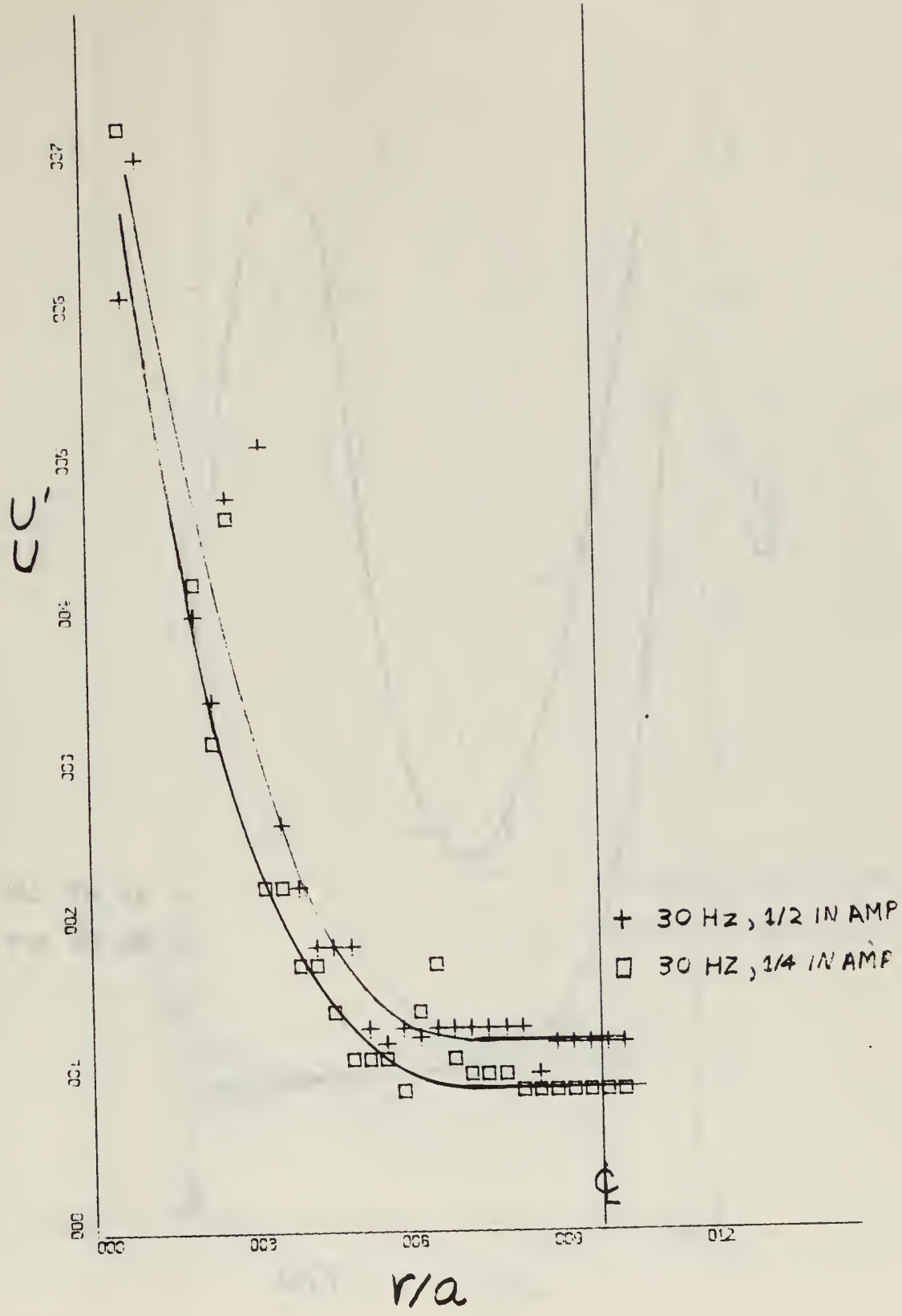

Figure 6: Radial Distribution of Disturbance Amplitude; z/d 16, R 5700

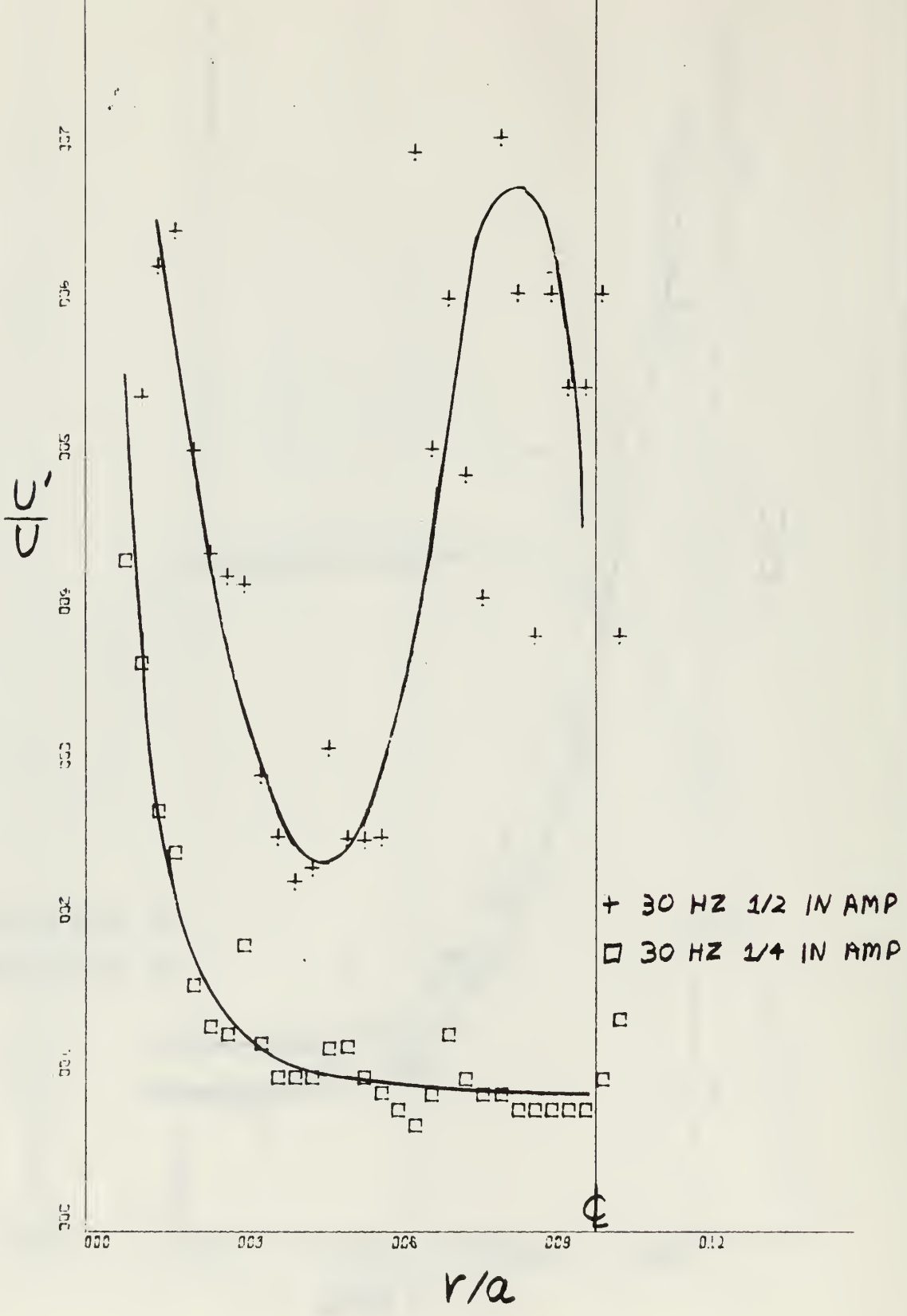

Figure 7: Radial Distribution of Disturbance Amplitude; z/d 48, R 5700

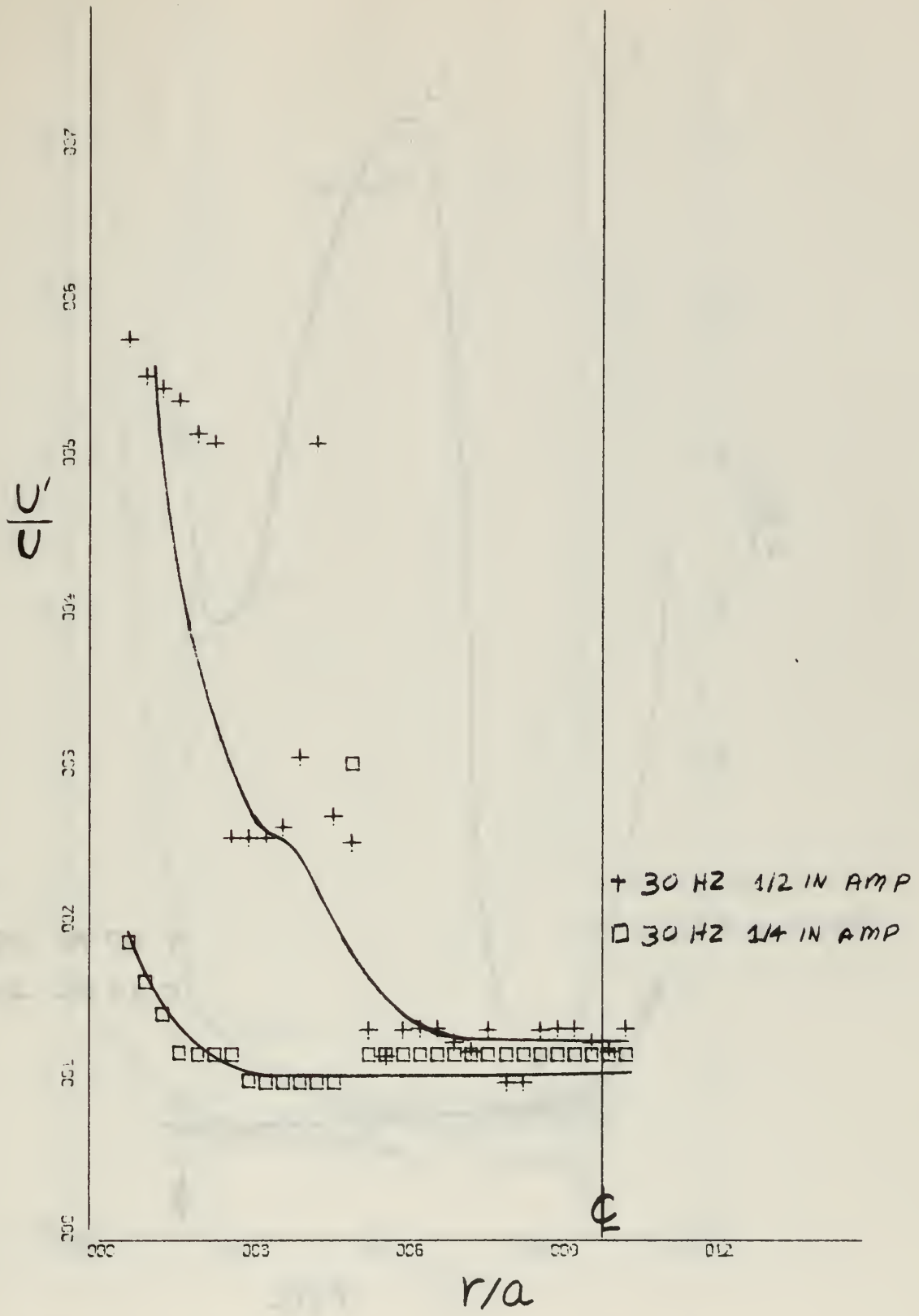

Figure 8: Radial Distribution of Disturbance Amplitude; z/d 16, R 8500

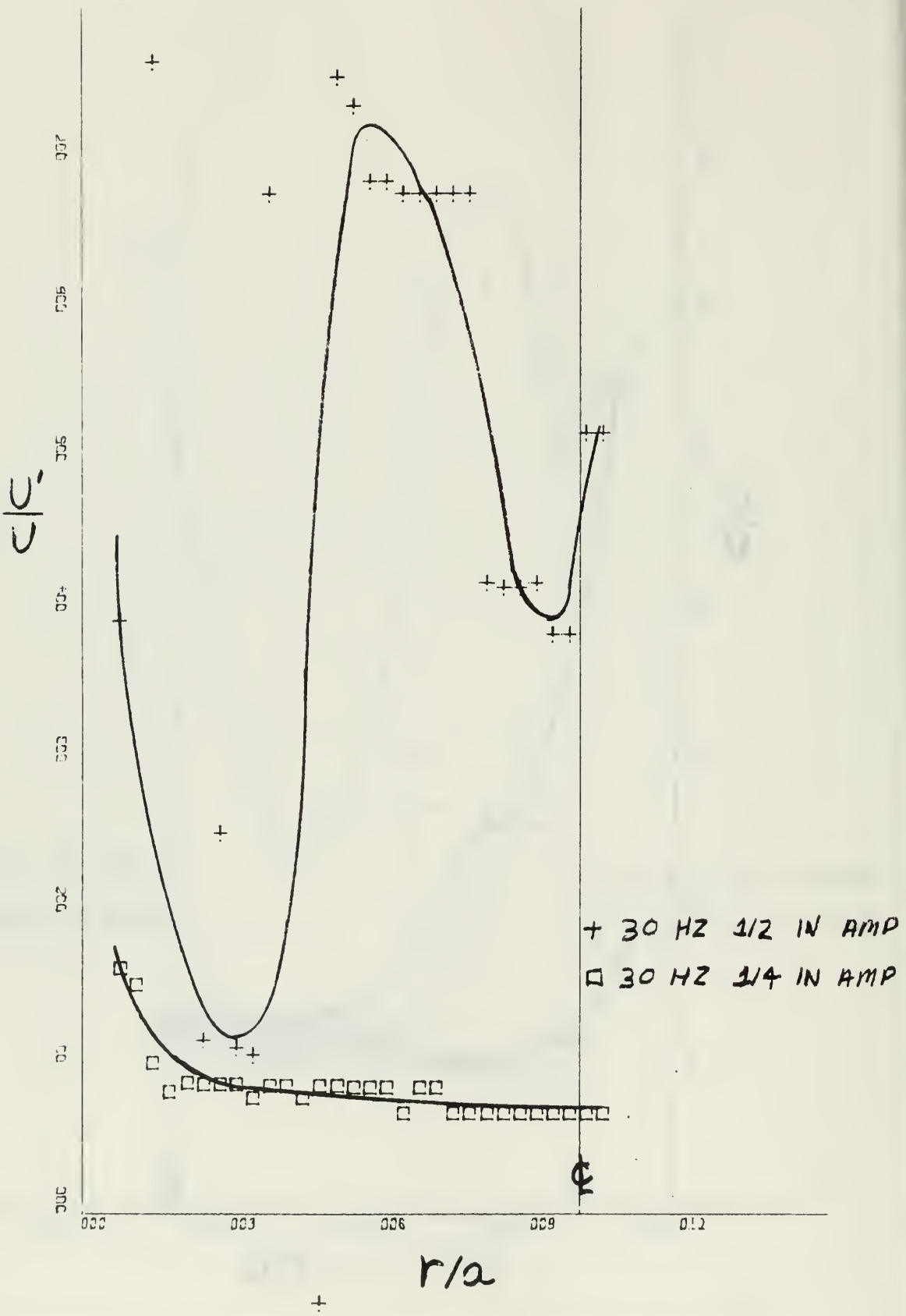

Figure 9: Radial Distribution of Disturbance Amplitude; z/d 48, R 8500

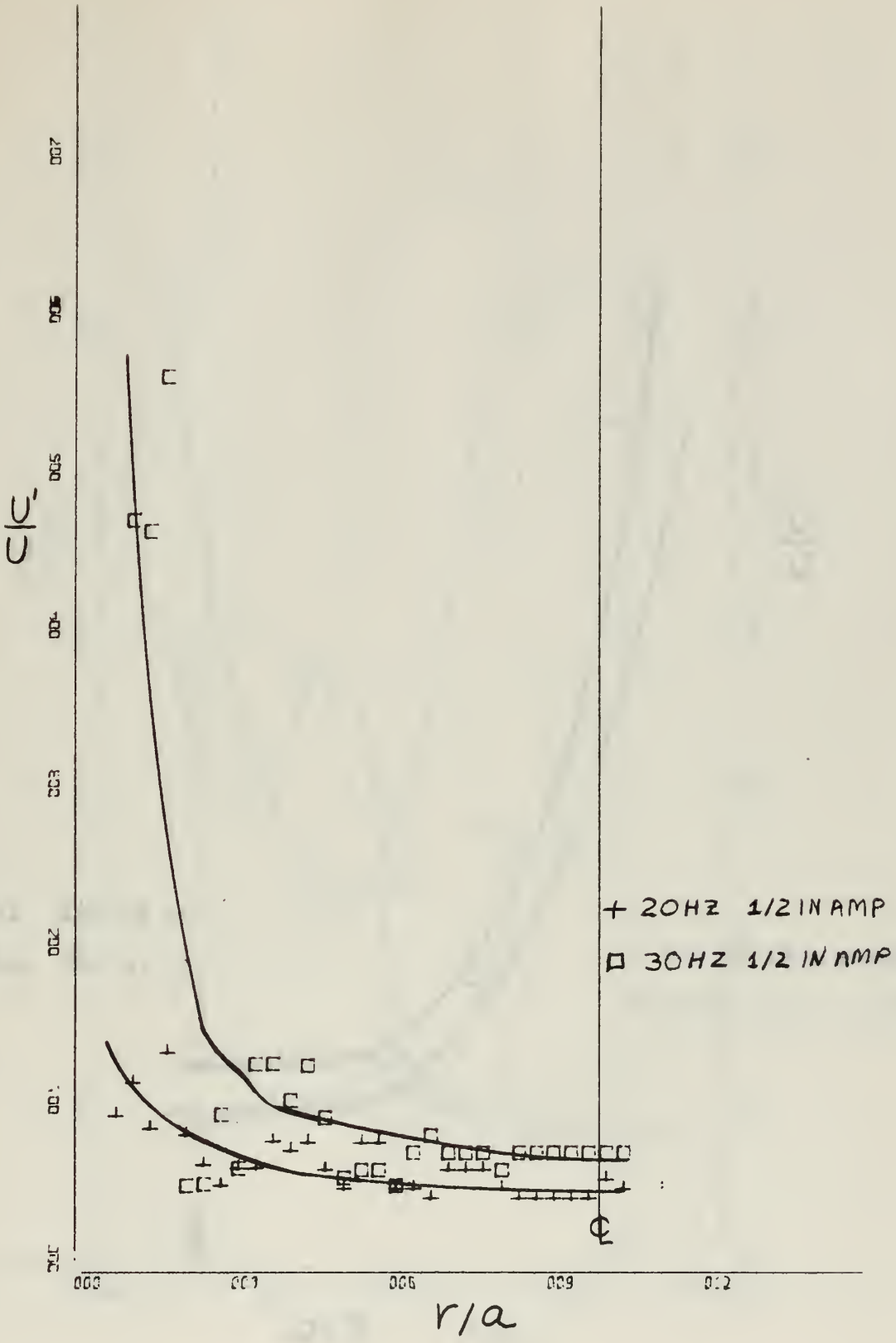

Figure 10: Radial Distribution of Disturbance Amplitude; z/d 56, R 5700, R 8500

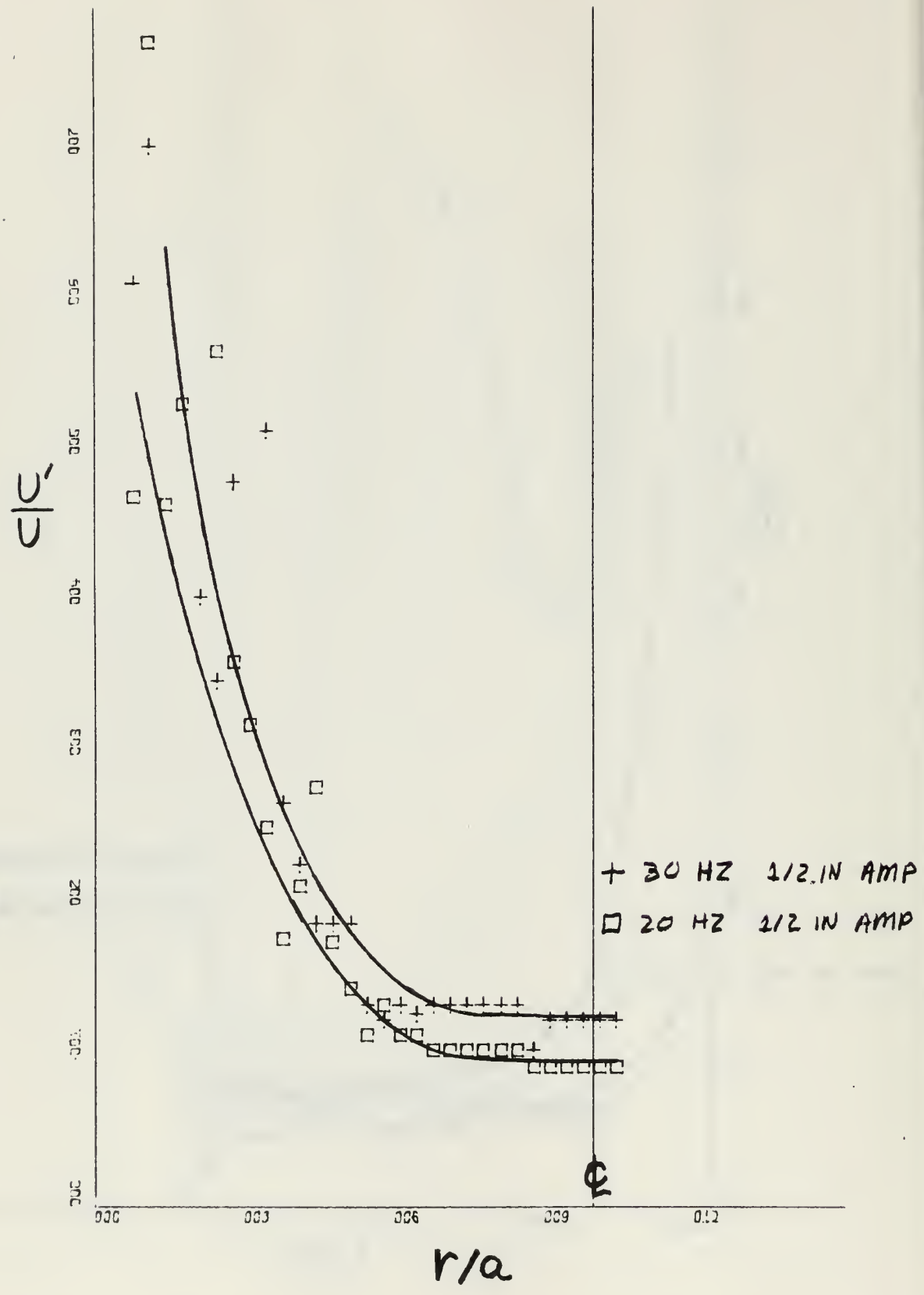

Figure 11: Radial Distribution of Disturbance Amplitude; z/d 16, R 5700

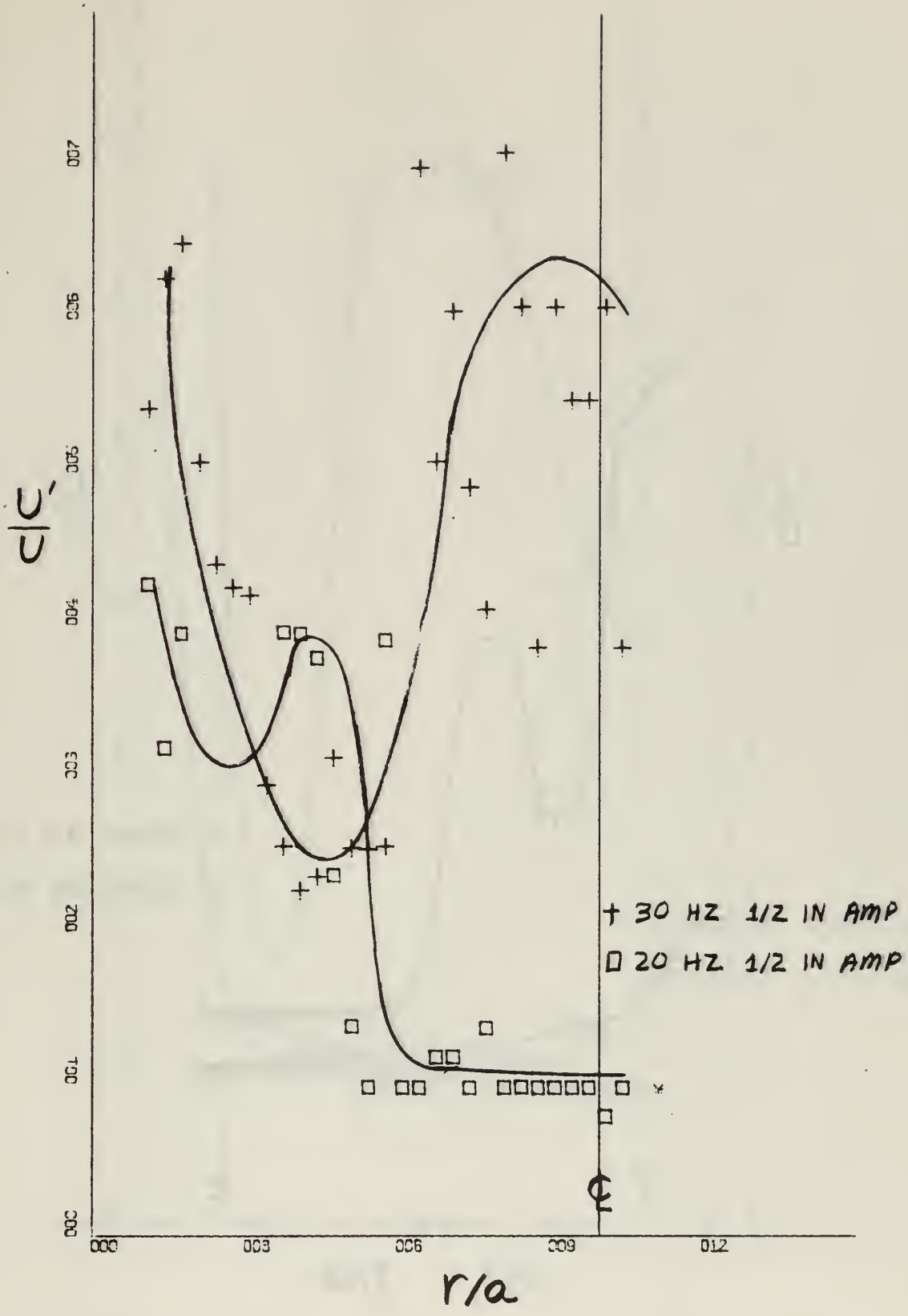

Figure 12: Radial Distribution Of Disturbance Amplitude; z/d 48, R 5700

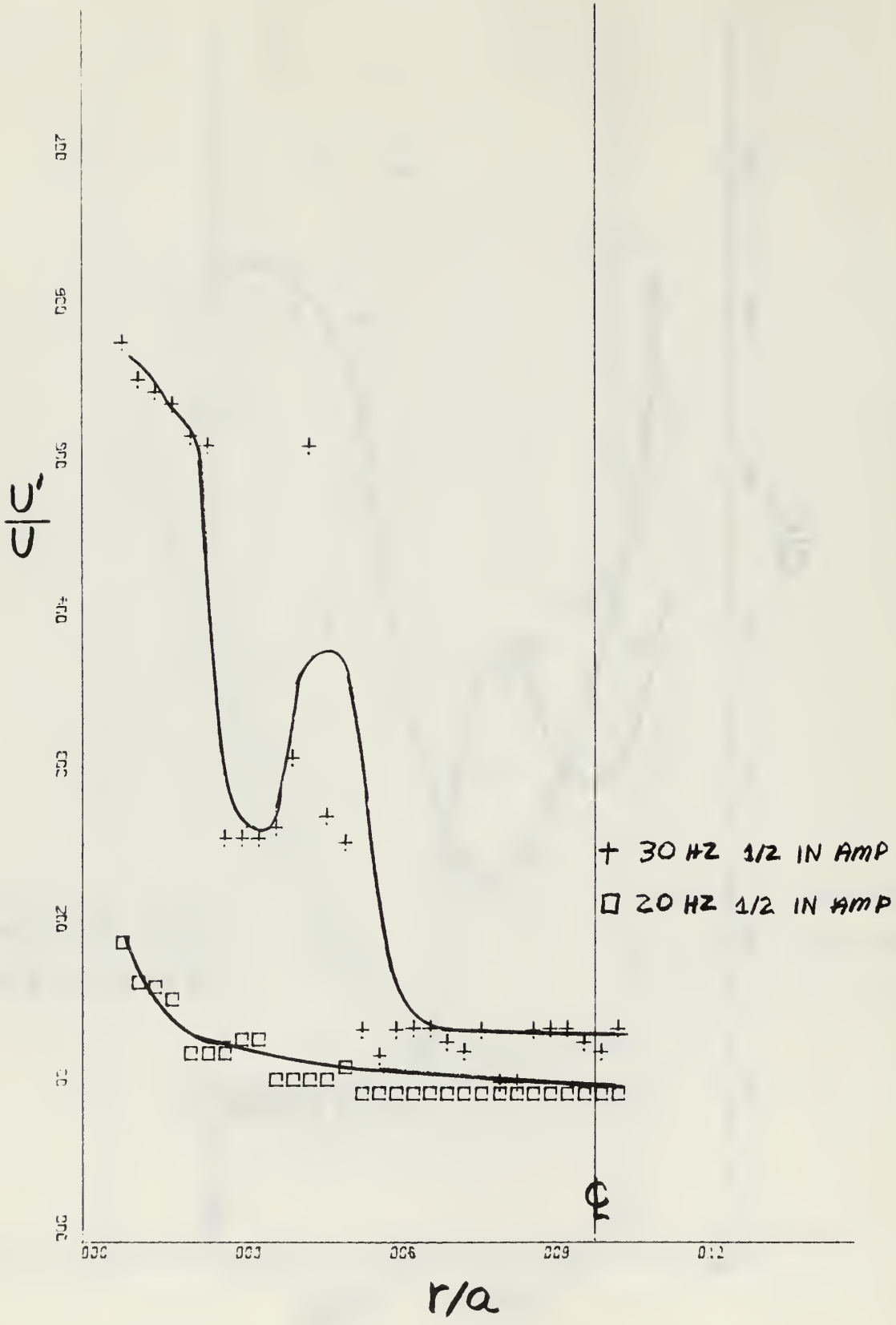

Figure 13: Radial Distribution of Disturbance Amplitude; z/d 16, R 8500

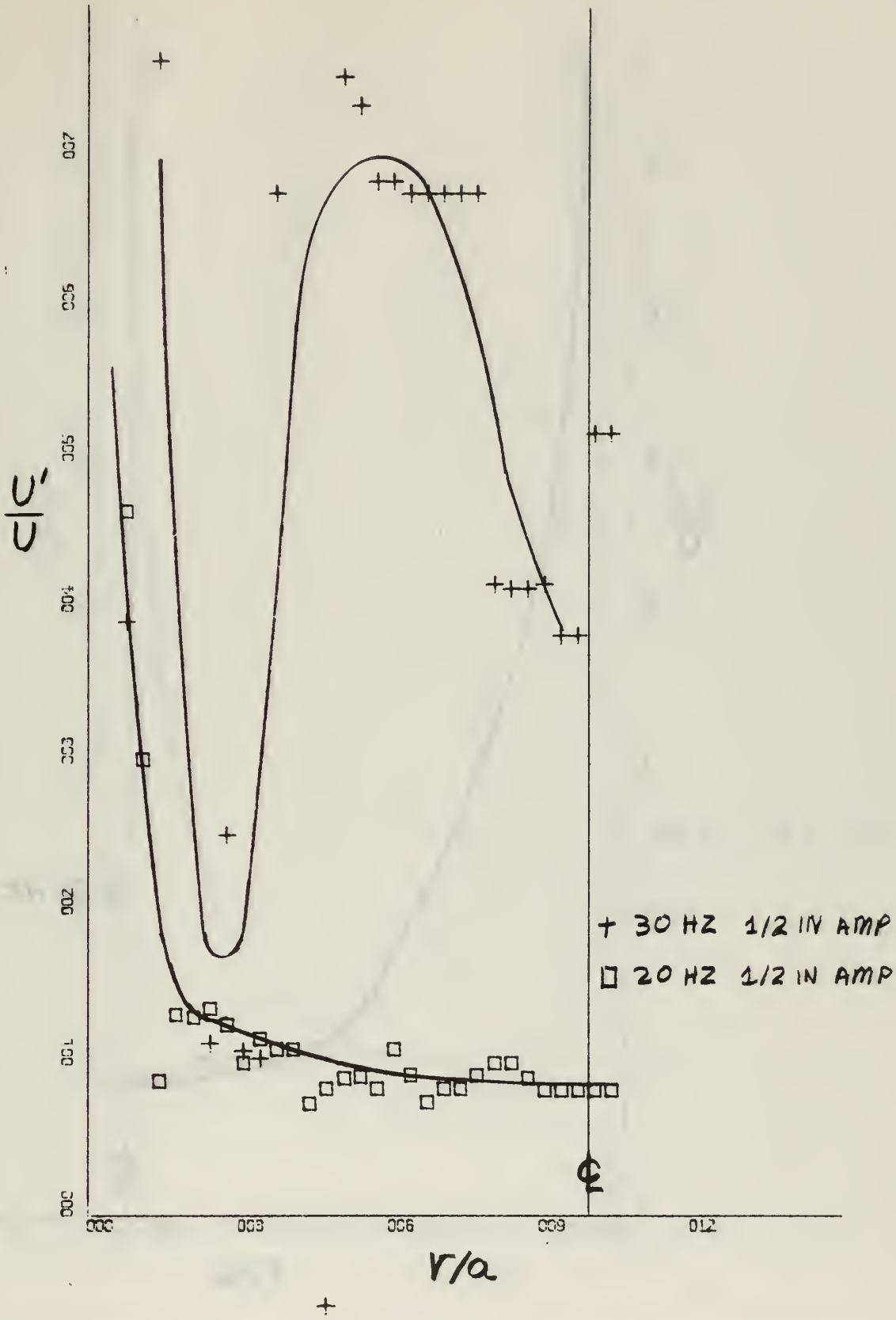

Figure 14: Radial Distribution of Disturbance Amplitude; z/d 48, R 8500

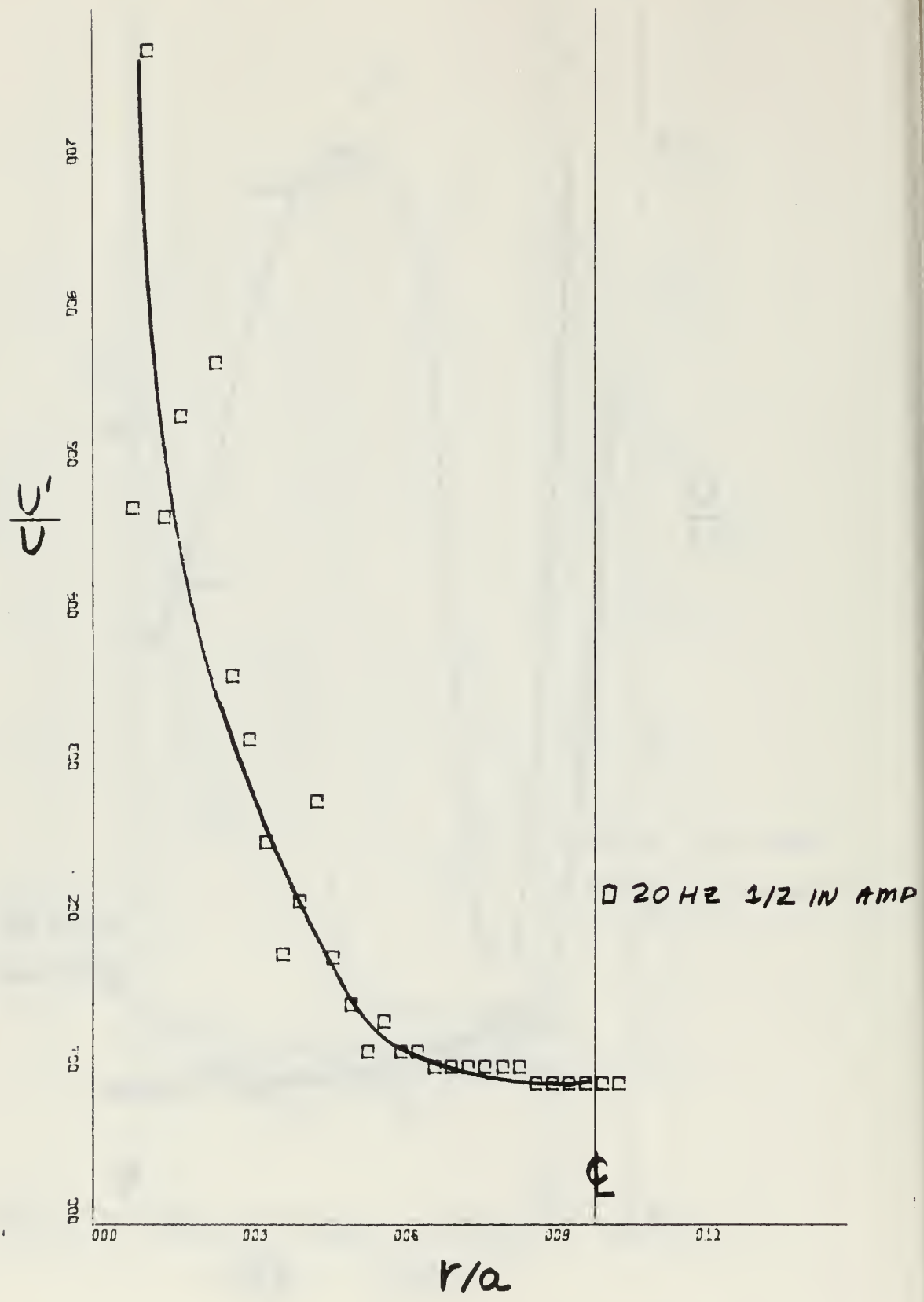

Figure 15: Radial Distribution of Disturbance Amplitude; z/d 16, R 5700

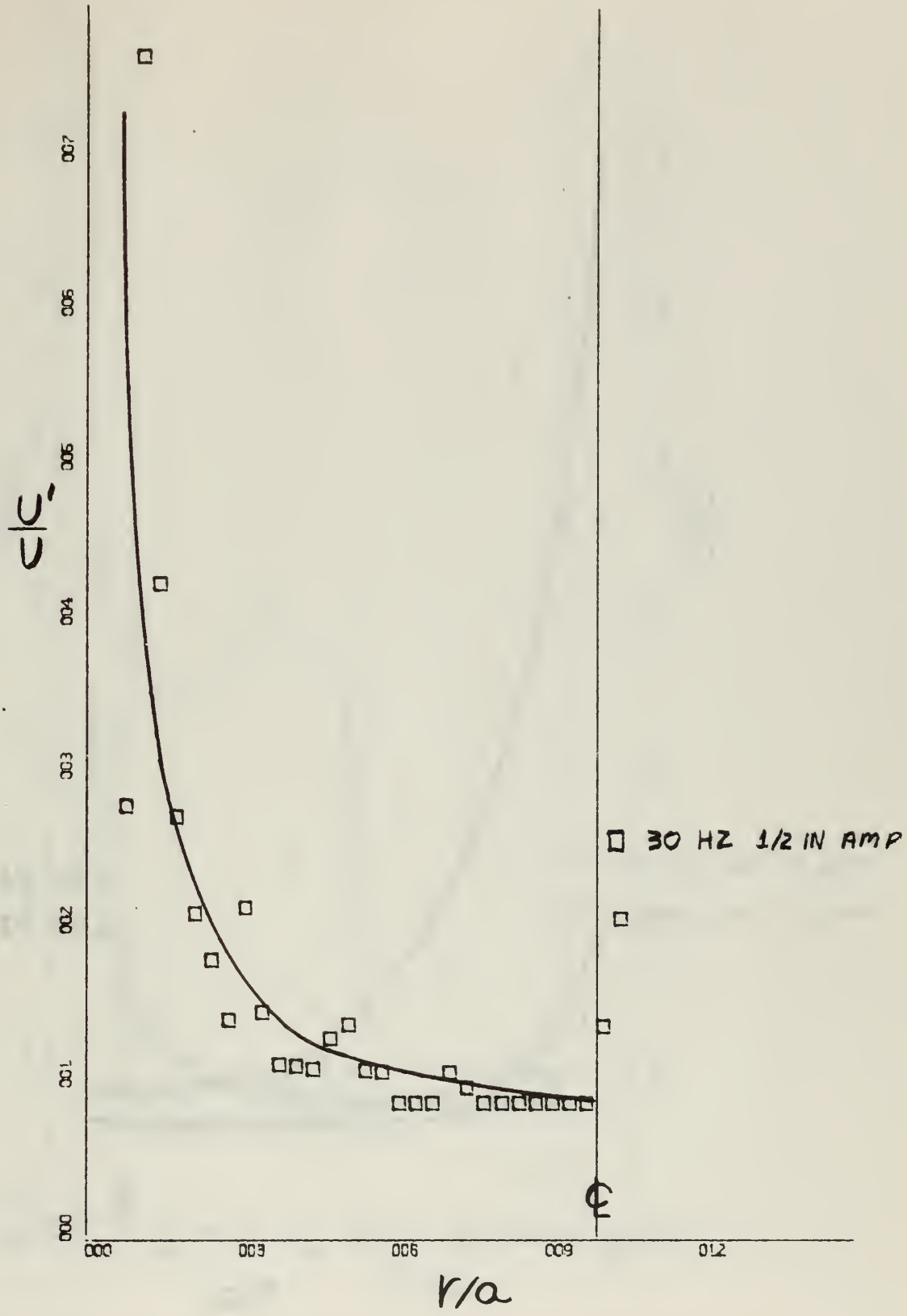

Figure 16: Radial Distribution of Disturbance Amplitude; z/d 32, R 5700

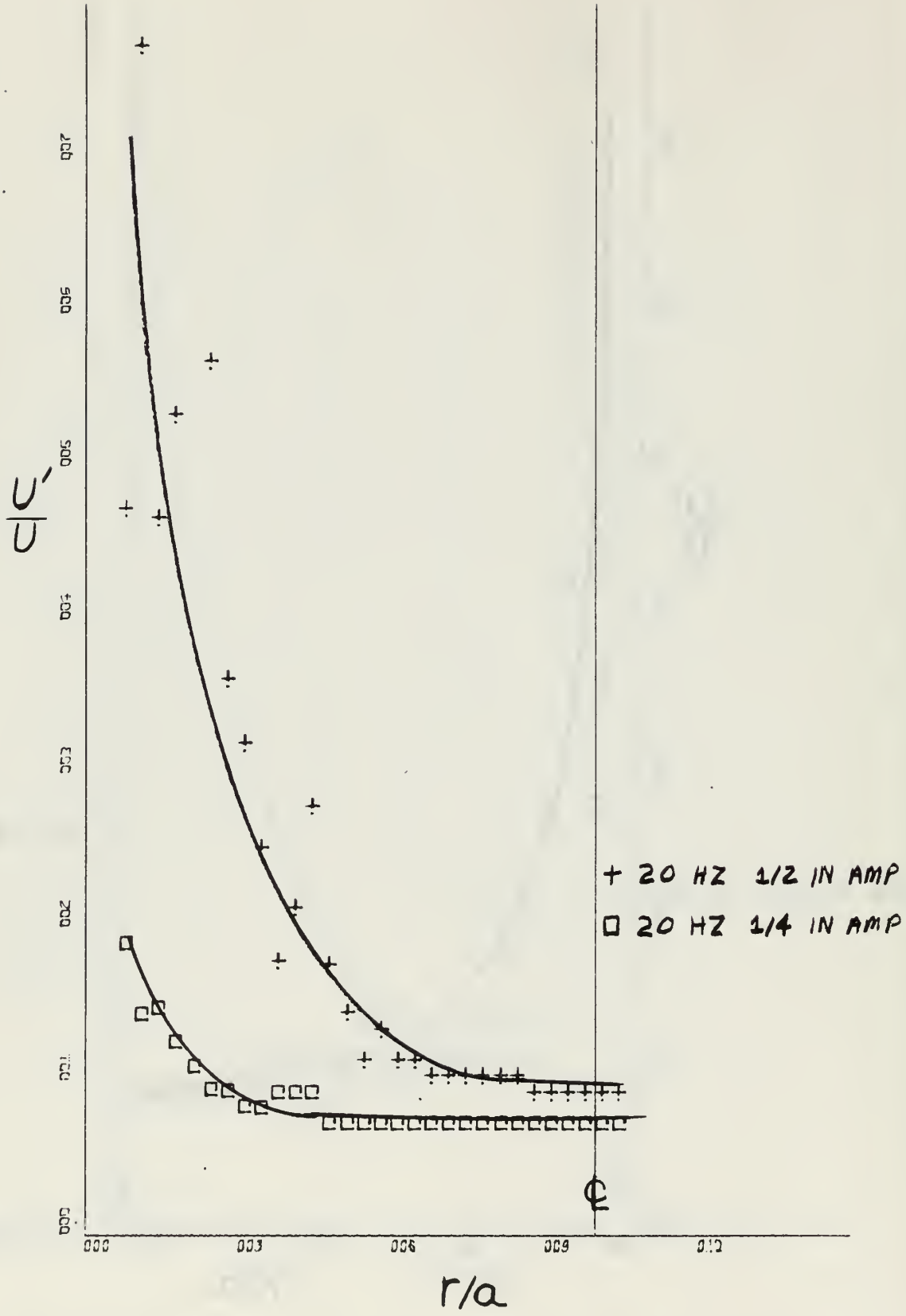

Figure 17: Radial Distribution of Disturbance Amplitude; z/d 16, R 5700

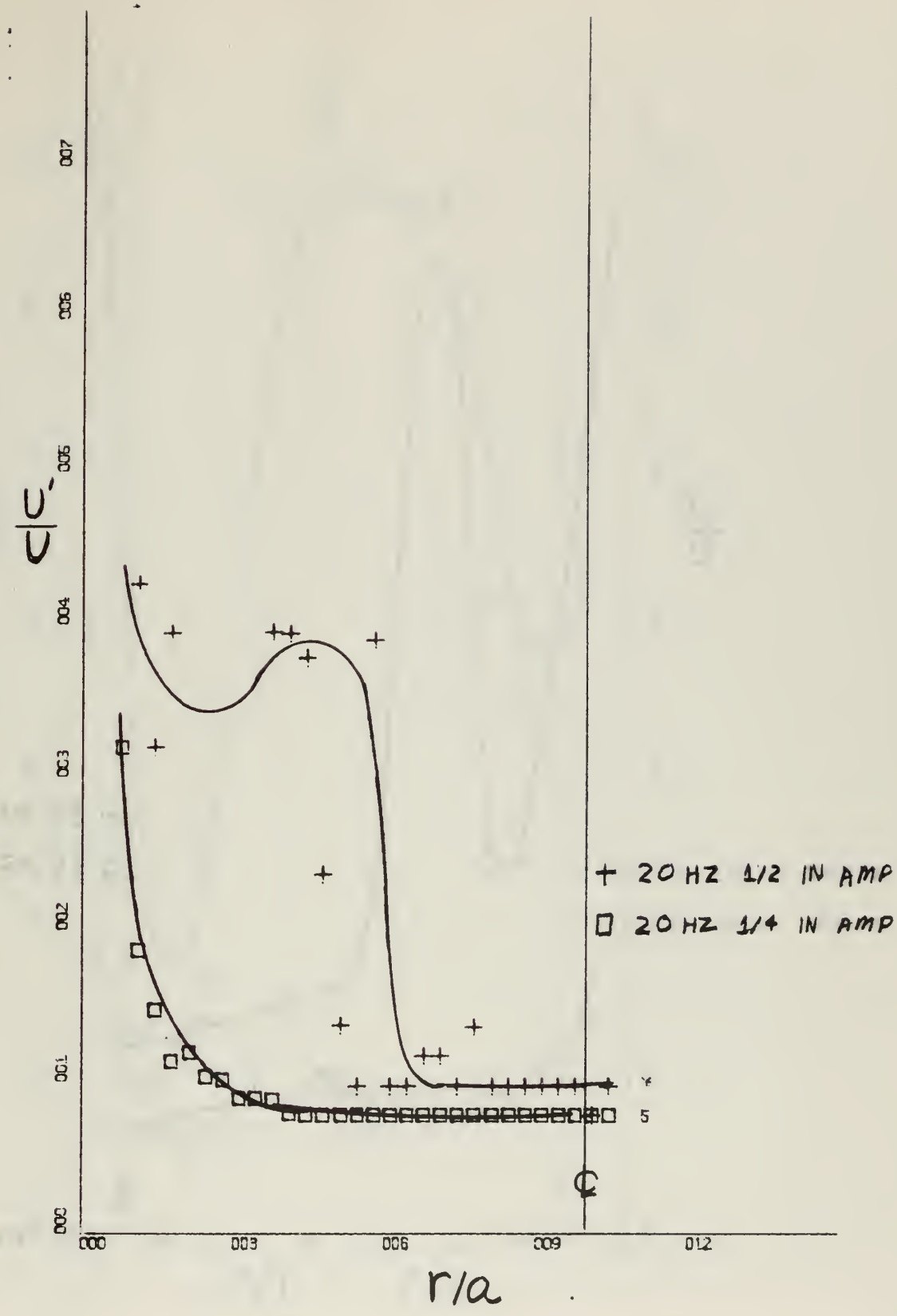

Figure 18: Radial Distribution of Disturbance Amplitude; z/d 48, R 5700

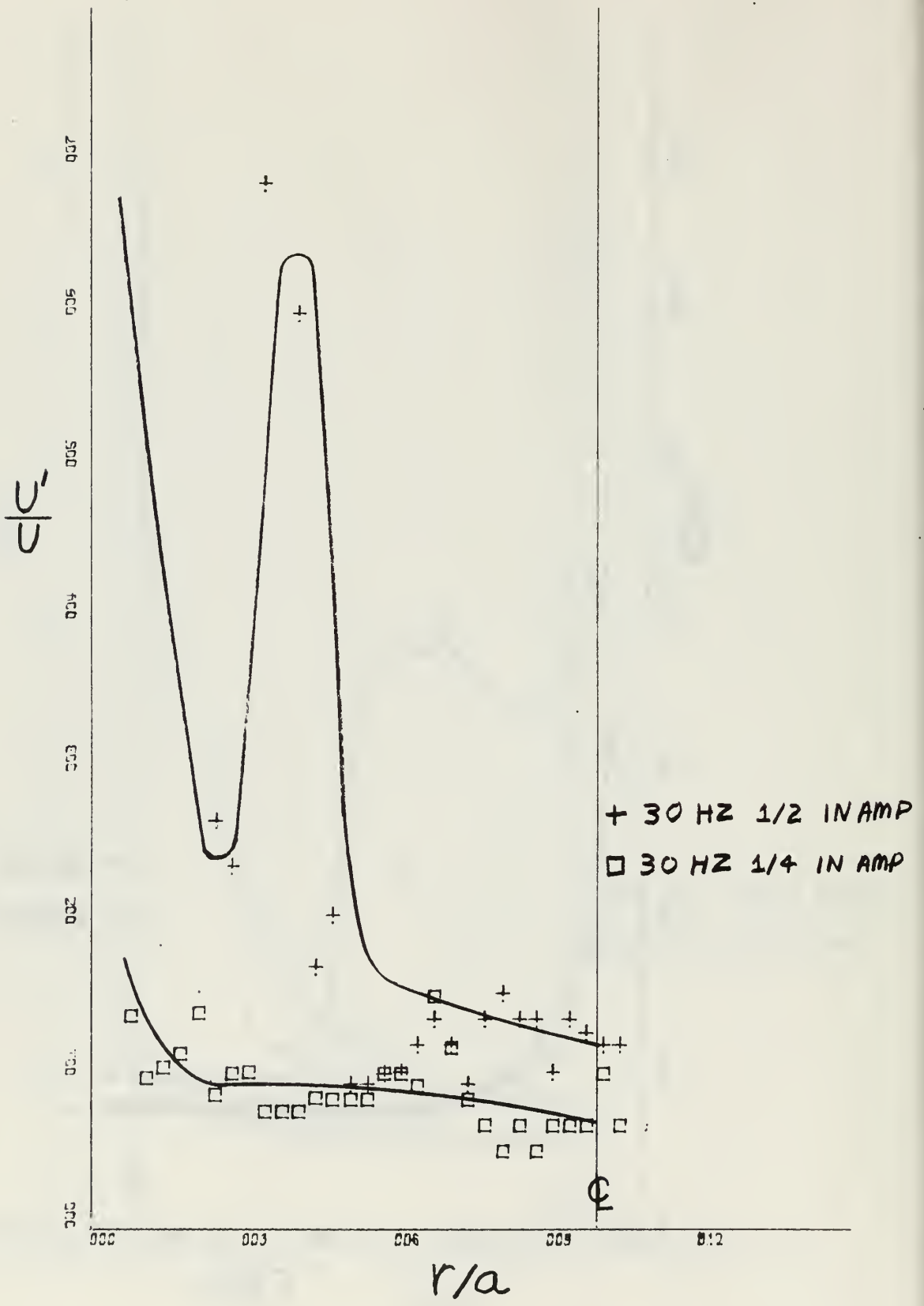

Figure 19: Radial Distribution of Disturbance Amplitude; z/d 32, R 8500

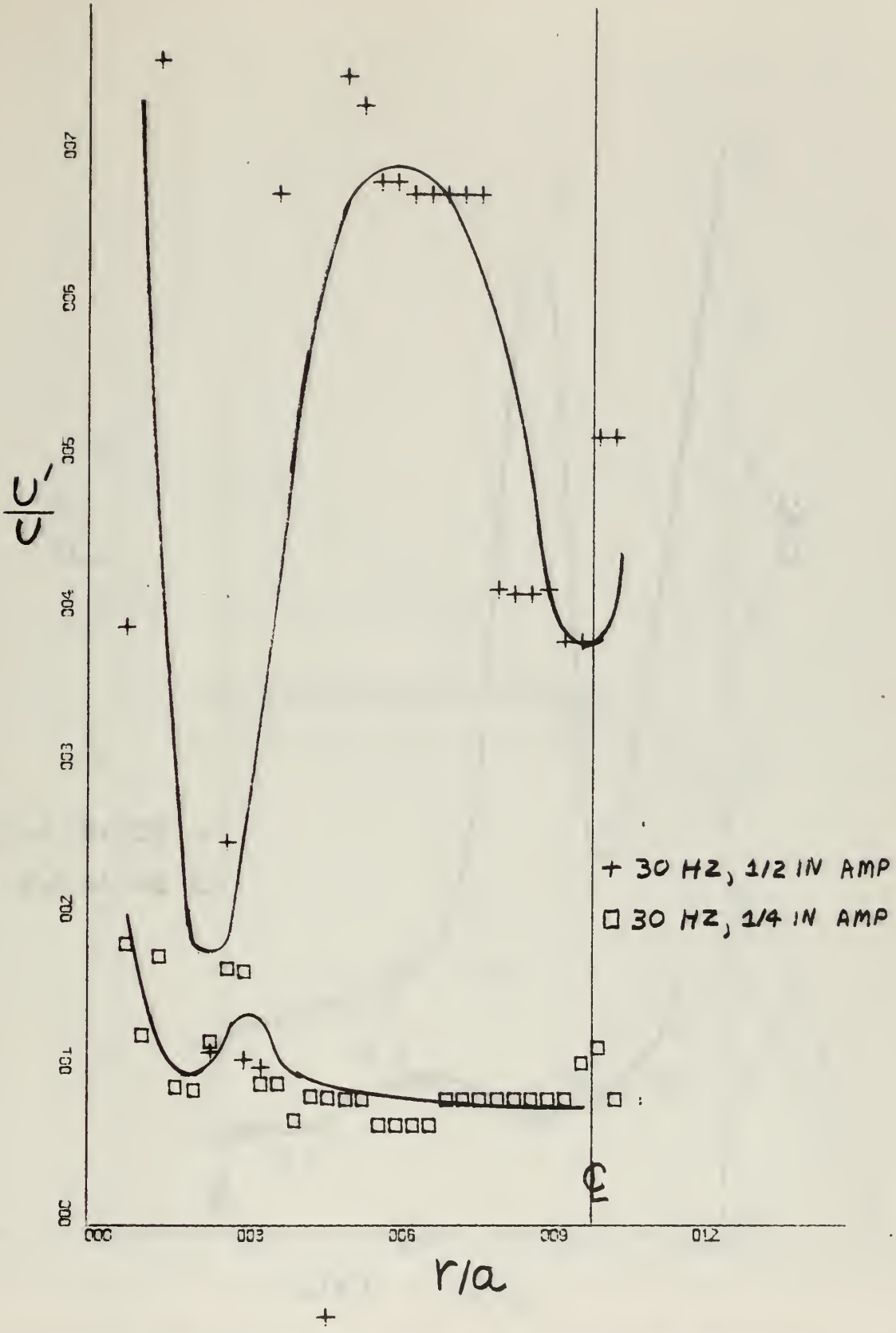

Figure 20: Radial Distribution of Disturbance Amplitude; z/d 48, R 8500

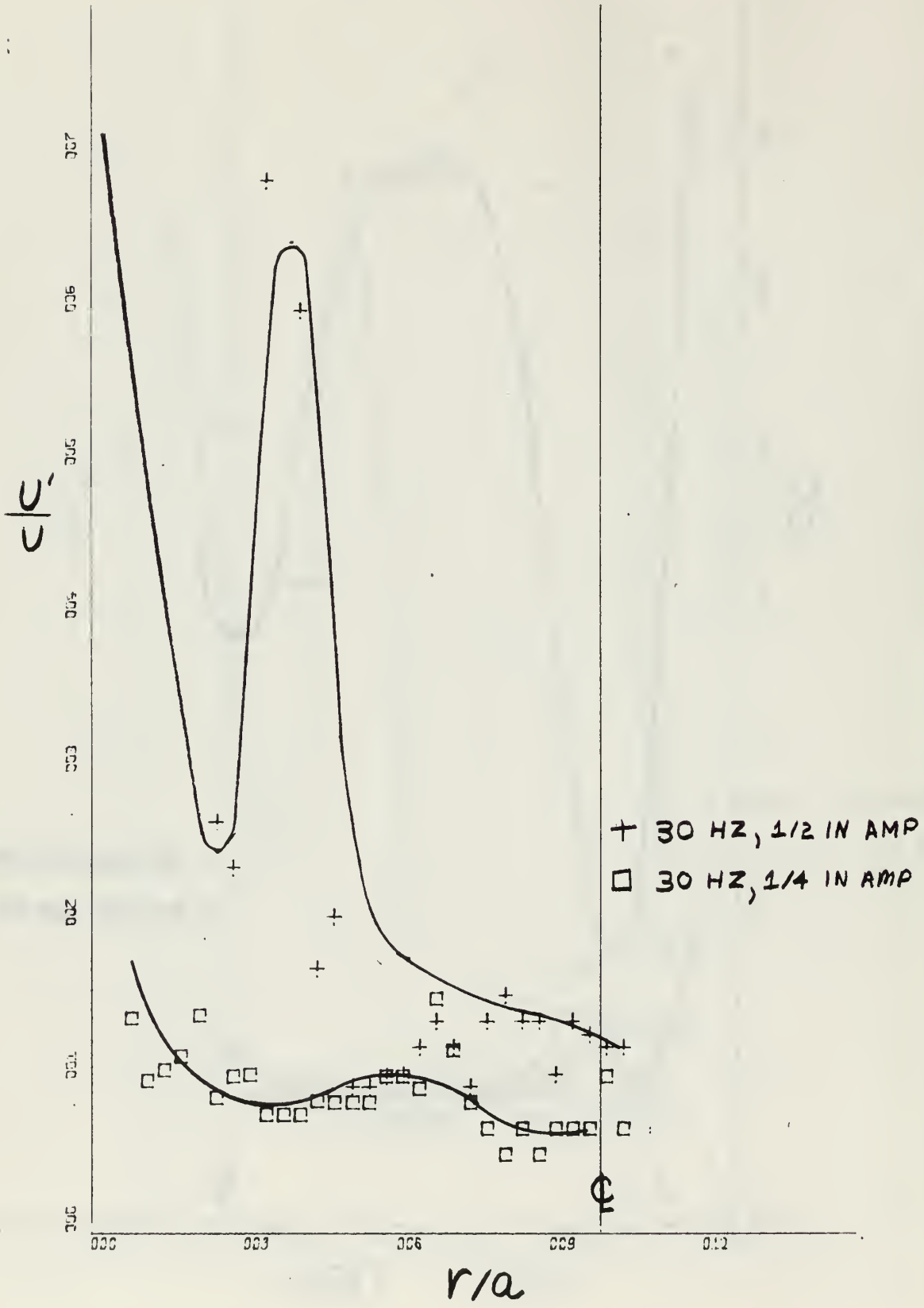

Figure 21: Radial Distribution of Disturbance Amplitude; z/d 32, R 8500

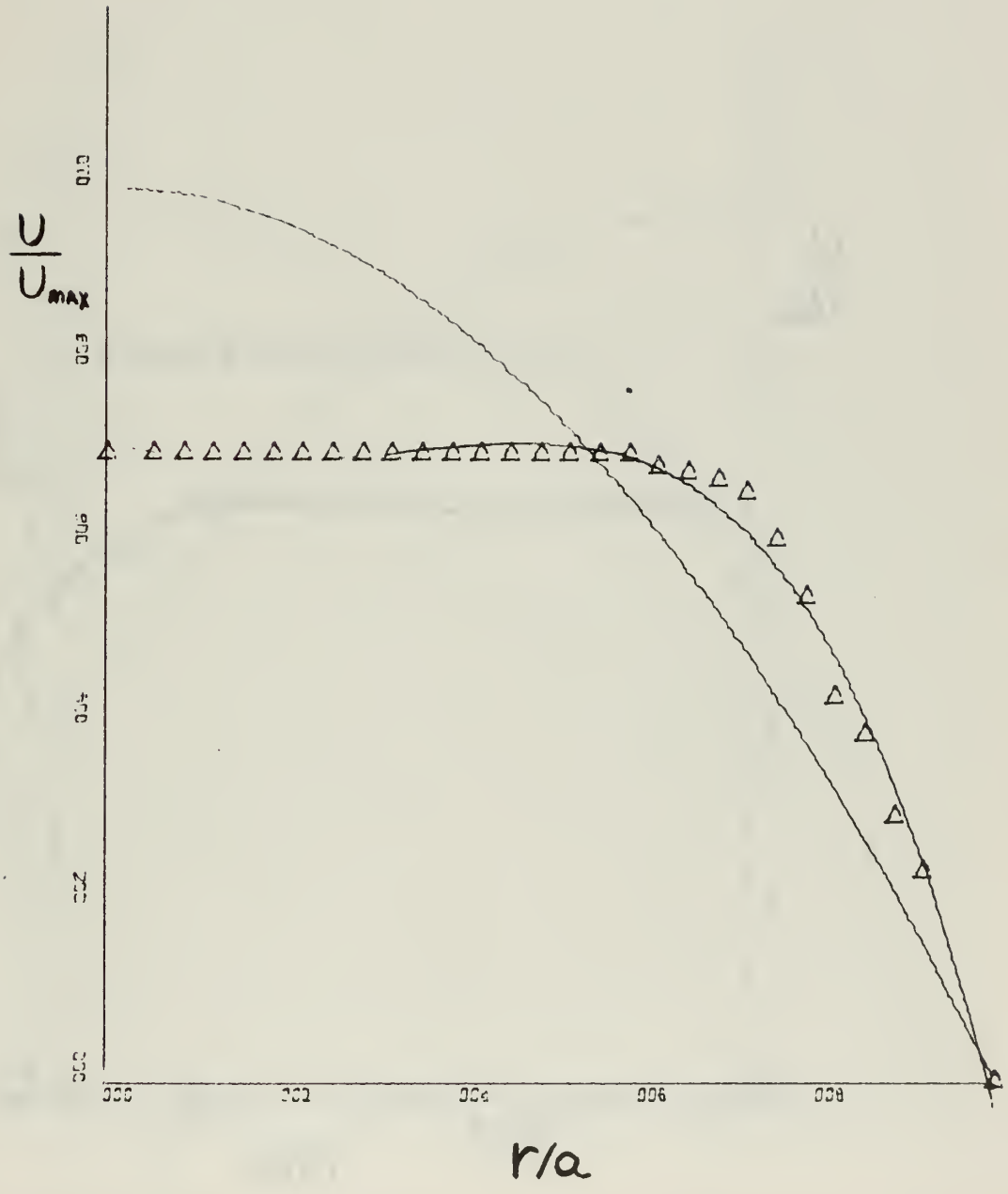

Figure 22: Polynomial Approximation to the Velocity Profile; z/d 16, R 5700

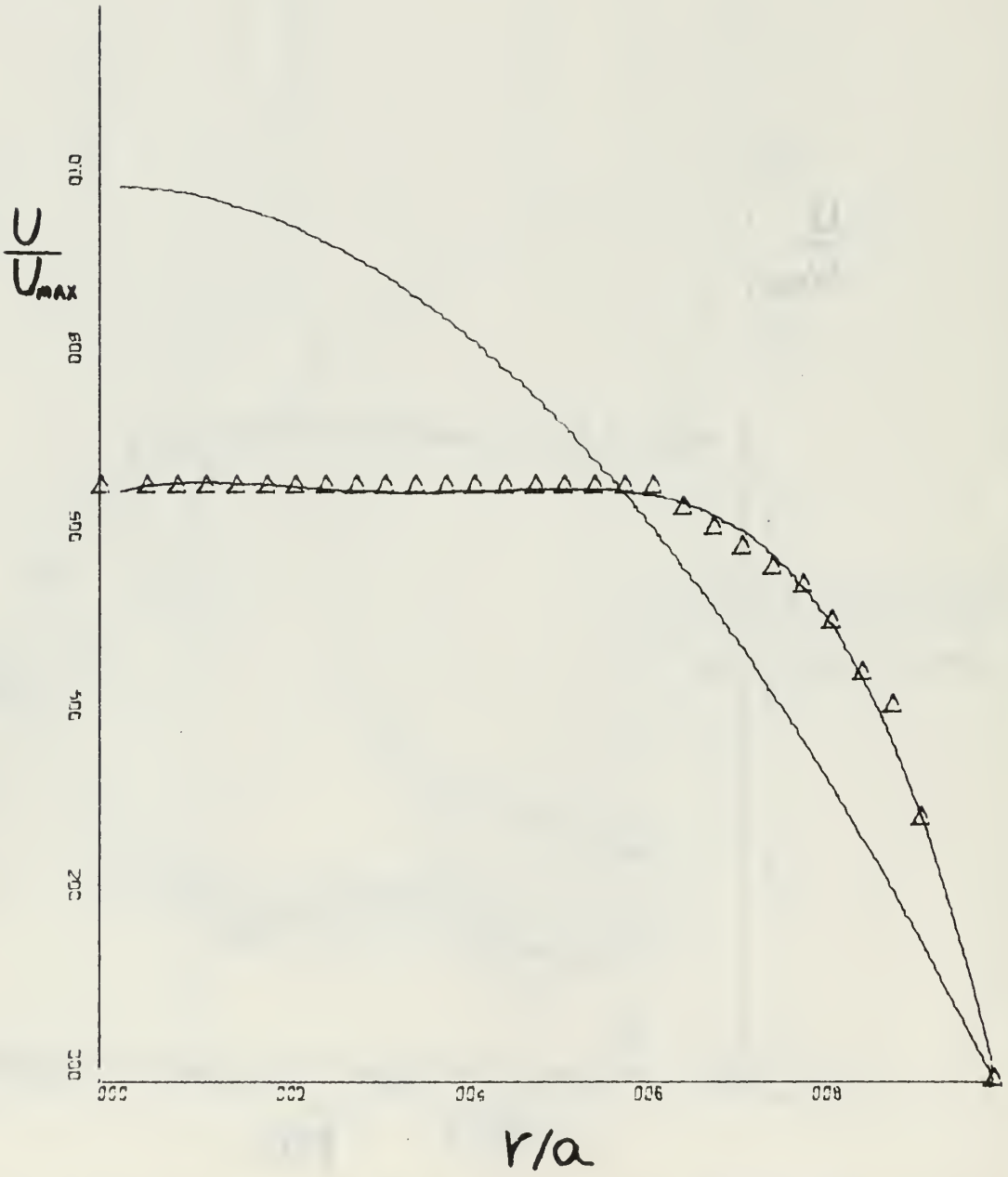

Figure 23: Polynomial Approximation to the Velocity Profile; z/d 56, R 5700

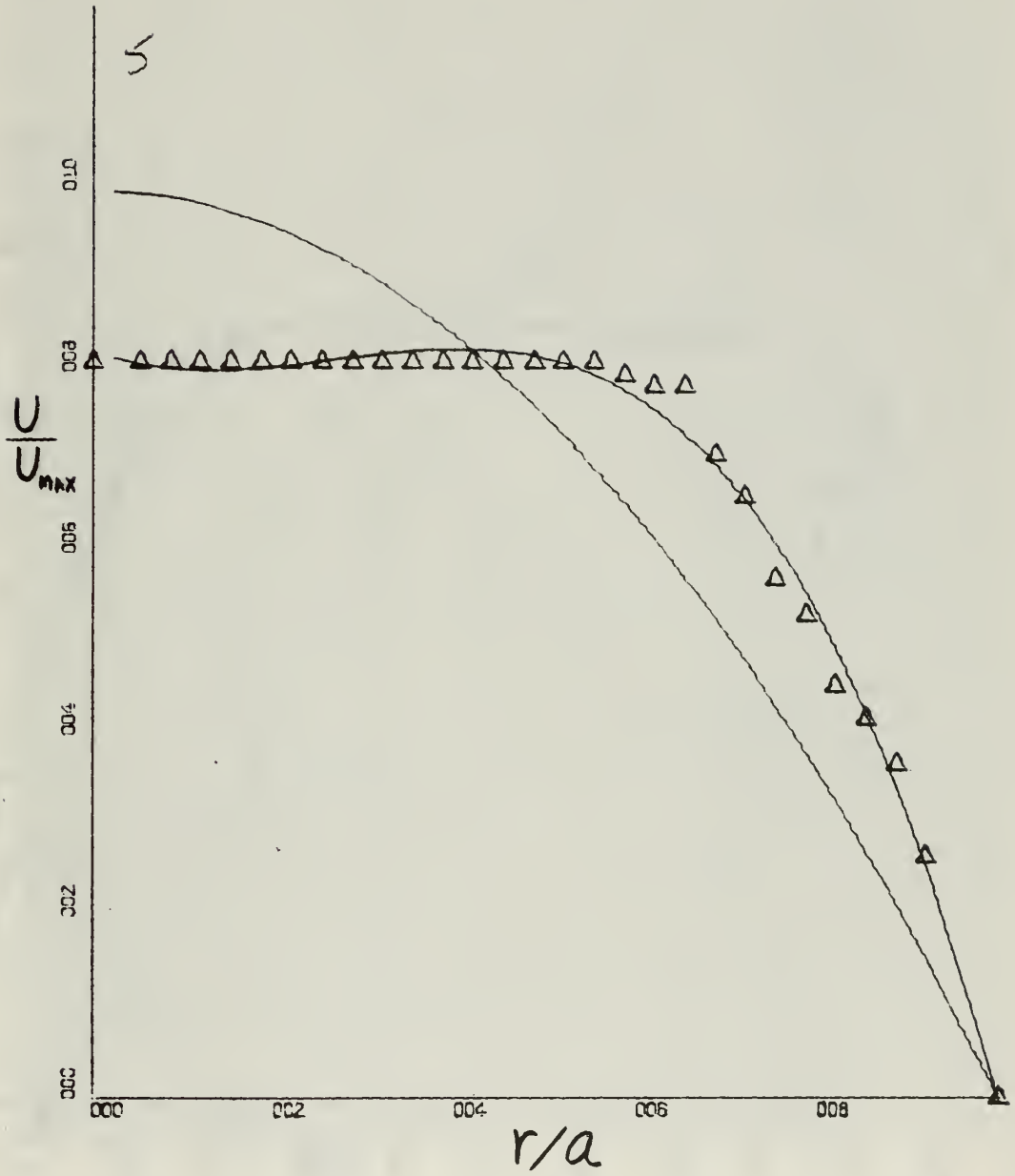

Figure 24: Polynomial Approximation to the Velocity Profile; z/d 16, R 8500

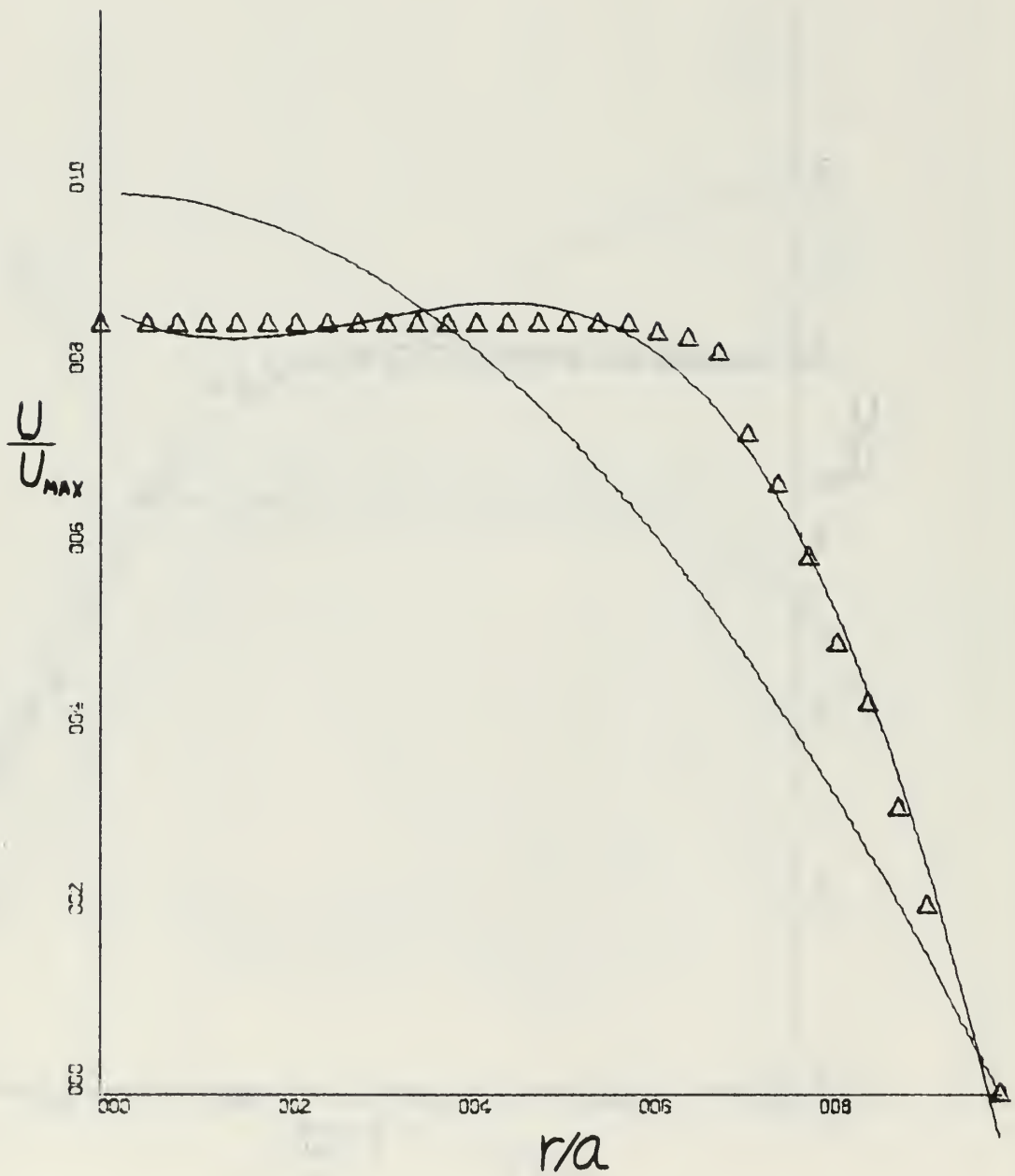

Figure 25: Polynomial Approximation to the Velocity Profile; z/d 56, R 8500

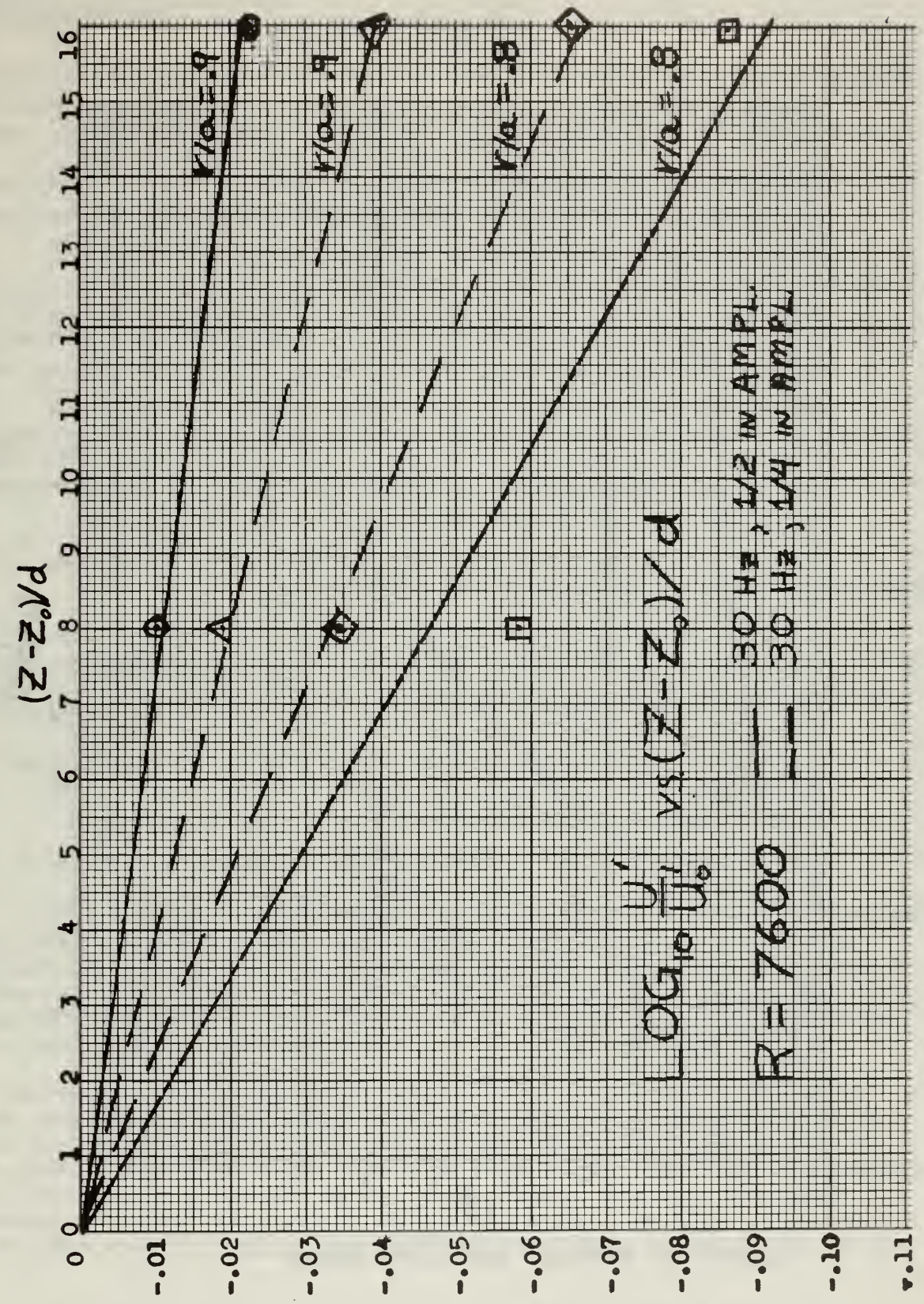

Figure 26: Decay of Disturbance Amplitude, R 7600

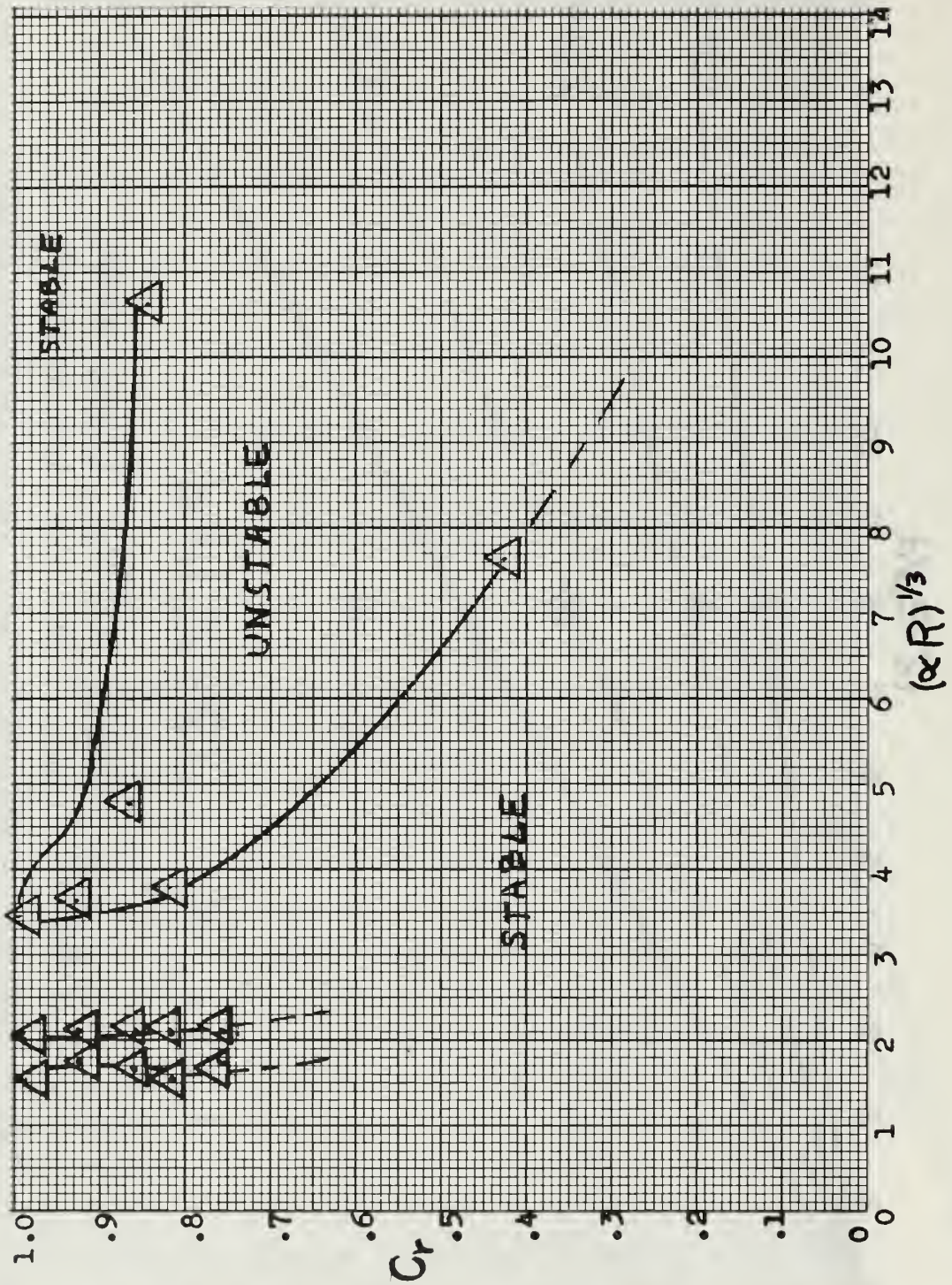

Figure 27: Neutral Stability Curve

DOCUMENT CONTROL DATA - R & D

(Security classification of title, body of abstract and indexing annotation must be entered when the overall report is classified)

1. ORIGINATING ACTIVITY *(Corporate author)*
Naval Postgraduate School
Monterey, California 93940

2a. REPORT SECURITY CLASSIFICATION
Unclassified

2b. GROUP

3. REPORT TITLE
An Experimental Investigation of the Stability of Poiseuille Flow

4. DESCRIPTIVE NOTES *(Type of report and inclusive dates)*
Master's Thesis; December 1969

5. AUTHOR(S) *(First name, middle initial, last name)*
Richard Evans Westbrook

6. REPORT DATE
December 1969

7a. TOTAL NO. OF PAGES
64

7b. NO. OF REFS
8

8a. CONTRACT OR GRANT NO.

b. PROJECT NO.

c.

d.

9a. ORIGINATOR'S REPORT NUMBER(S)

9b. OTHER REPORT NO(S) *(Any other numbers that may be assigned this report)*

10. DISTRIBUTION STATEMENT
This document has been approved for public release and sale, its distribution is unlimited.

11. SUPPLEMENTARY NOTES

12. SPONSORING MILITARY ACTIVITY
Naval Postgraduate School
Monterey, California 93940

13. ABSTRACT

A theoretical and experimental investigation of the stability of developing laminar flow in a circular pipe subjected to small, rotationally symmetric (torsional) disturbances is presented. Analytically, developing mean velocity profiles were represented in polynomial series form and subsequent formulations yielded determinations on stability which reduce to the classical conclusions for the case of fully developed flow.

Experimentally, torsional disturbances were imposed upon a developing laminar pipe flow by sinusoidally rotating a 1.5 inch (1 diameter) length of pipe in the entrance region of a carefully constructed wind tunnel facility. For flows with maximum Reynolds numbers of 8500, maximum amplitude and frequency of oscillation were ½ inch and 30 Hz., respectively. Hot wire anemometer measurements verified the stability of the developing flow field. Moreover, measured wave speeds and decay factors compare favorably to calculated values.

14 KEY WORDS	LINK A		LINK B		LINK C	
	ROLE	WT	ROLE	WT	ROLE	WT
Stability of entry length pipe flow						
To torsional disturbances						